Additive Manufacturing 38 (2021) 101749

Contents lists available at ScienceDirect

Additive Manufacturing

journal homepage: www.elsevier.com/locate/addma

Review

In situ monitoring for fused filament fabrication process: A review

Yanzhou Fu [a,*,1], Austin Downey [a,b,2], Lang Yuan [a,3], Avery Pratt [c], Yunusa Balogun [c]

[a] Department of Mechanical Engineering, University of South Carolina, Columbia, SC 29201, United States
[b] Department of Civil and Environmental Engineering, University of South Carolina, Columbia, SC 29201, United States
[c] Naval Surface Warfare Center (Crane Division), Crane, IN 47522, United States

ARTICLE INFO

Keywords:
Additive manufacturing
Fused filament fabrication
3D printing
Monitoring system

ABSTRACT

Real-time monitoring of the additive manufacturing process offers the promise of guaranteeing product quality and increasing the efficiency of the printing process. This paper summarizes research results for the in situ monitoring of the printing process for the fused filament fabrication process. To have a systematic and comprehensive summary, different methods, devices, and achievements in a range of monitoring systems for 3D printing are described. Sensor types and devices used in the literature for printer health-state monitoring and printing process product quality monitoring are summarized. Discussion of current and future research directions concludes the review.

1. Introduction

Additive manufacturing (AM) is actively used in a variety of industries. According to the Wohlers Report on additive manufacturing in 2020 it shows enormous economic potential [1,2]. The revenue is expected to rise to $23.9 billion in 2022 for all AM products and services worldwide. It is further predicted to climb to $35.6 billion in 2024 [3]. The printing process of AM is typically stacking material layer-by-layer to build three-dimensional (3D) products. Due to the advantages of low production lead time and the ability to create complicated geometries and shapes, the process has been employed for various industrial applications. One of the fastest-growing and widely-used AM technologies is fused filament fabrication (FFF) [4]. During the FFF process, the thermoplastic filament is fed into a hot end that melts the material and extrudes it from the nozzle onto a build platform, which forms a thin cross-sectional layer or track. This process is repeated until the whole object is fully printed. The most common FFF thermoplastic filaments are acrylonitrile butadiene styrene (ABS) and polylactic acid (PLA) [5], while polycarbonate (PC), polyetherimide (Ultem), polyphenylsulfone (PPSF), nylon, and polyether ketone ketone (PEKK) are also used in industrial settings [6]. FFF has been utilized for various applications, including biomedical [7], civil [8], and medical [9,10], in addition to being explored by hobbyists and educators [2,11,12].

Despite its advantages, FFF has lower reliability than other manufacturing processes, including other AM processes such as stereolithography (SLA) [13], selective laser sintering (SLS) [14], and laminated object manufacturing (LOM) [15]. Previous research estimates a 20% printing failure rate for FFF by unskilled users [16]. These reliability statistics arise from challenges related to material runout, nozzle clogging, excessive vibration, over-extrusion or under-extrusion, and defects associated with temperature validation. In addition, the FFF process is very sensitive to environmental conditions [17–19]. Better temperature settings, more uniform filament quality, and novel filament feed system could improve the printing process [20–22]. Furthermore, robust closed-loop control of the FFF process could mitigate process variations [23,24]. Active control of the printing process will become critical as the size and complexity of fabricated parts increase.

In general, there are two forms of quality monitoring for the FFF process: (1) monitoring of printer health state; and (2) detecting product defects during the printing process. Ensuring high printer health state is key to guarantee printing efficiency and product quality [119]. Researchers have investigated the use of sensors, such as vibration sensors, acoustic emission (AE) sensors, accelerometers, infrared thermometers, and visual cameras for monitoring printer health state [120]. Beyond monitoring the printer's health state, in situ printing process defect monitoring is indispensable for detecting product quality defects [73,

* Corresponding author.
E-mail address: yanzhouf@email.sc.edu (Y. Fu).
[1] Yanzhou Fu:0000-0002-5471-9972
[2] Austin Downey:0000-0002-5524-2416
[3] Lang Yuan:0000-0002-6894-5030

https://doi.org/10.1016/j.addma.2020.101749
Received 26 July 2020; Received in revised form 17 November 2020; Accepted 2 December 2020
Available online 17 December 2020

121]. Here, the vast majority of research has focused on combining images taken during the printing process with image analysis, machine learning (ML), or other defect detection algorithms. Table 1 is a compilation of sensors and devices from the literature which are used for monitoring the 3D printer's health state, monitoring the printing process product quality, or both.

The purpose of this paper is to review and summarize the research that has been done on monitoring of the FFF printing process, examine the impacts of these monitoring systems, and discuss the current and future research direction. In this paper, the background is described in Section 1, and Section 2 presents different ways and devices used for monitoring 3D printer health conditions. In Section 3, research that focuses on monitoring the product quality during the printing process is discussed, the conclusion and future trends are provided in Section 4. The interested reader is referred to [122–137] for a more detailed review on AM techniques in general or [5,138–140] for FFF and similar extrusion processes.

2. Monitoring and analysis of 3D printer health state in the printing process

For a consumer-grade FFF machine, Fig. 1a gives a generalized overview of the main components. In FFF, the extruder cold end drives the thermoplastic filament to the hot end, where it is heated until molten, then fed through the nozzle to bond it layer-by-layer on the heated build platform until the product is completed. In some cases, the platform is not heated and referred to as just a build platform [141]. By monitoring a 3D printer's health state during the printing process, machine downtime and material loss can be avoided. For the majority of FFF machines used by individuals and industry, the extruder and heated build platform are the two essential parts that, to a large extent, determine the success of printing [142]. Specific examples of conditions/parameters to be monitored include nozzle clogging, nozzle temperature, filament runout, and heated build platform temperature. The extruder is made up of two different parts: the cold end and the hot end. The details for these two components can be seen from Fig. 1b. The cold end drives the filament into the extruder's hot end and has two important components: the stepper motor and drive gear or hobbed bolt that drives the filament and the idler pulley shaft that holds the filament in the correct place during the extrusion process. When the filament arrives at the hot end, the components in the hot end (i.e., heater block, heat sink, heater cartridge, and thermocouple) work together to accurately heat the filament to a liquid state before extruding it from the nozzle [143]. Generally speaking, there are two extrusion systems available: direct extrusion and Bowden extrusion [144]. These vary by the location of the extruder's cold end. As the name implies, a direct extrusion system positions the cold end directly above the hot end. For Bowden extrusion, the cold end is most often mounted on the printer's body or frame, so that the filament feeds to the hot end through a Bowden tube [145]. Each of the extrusion type has pros and cons [146]. In direct extrusion, a benefit is the finer extrusion and retraction control due to the extruder's motor position directly over the hot end. Moreover, as less torque is needed to push the filament from the motor, smaller motors can be utilized. But with the extruder mounted adjacent to the print head, the total weight of the moving portion of the print head is increased. This extra weight adds constraints to printing speed, and it also causes wobbling and a potential loss of accuracy in the X and Y axis. For Bowden extrusion, since the extruder is fixed on the printer's frame, less weight is on the printing header. This results in higher printing accuracy and faster print speeds. However, the Bowden extruder needs to pull and push the filament through the long tube; therefore, greater friction exists in this process. Greater friction means a larger motor is required to supply the greater torque to drive the filament. And controlling the filament through the long tube also increases the response time. Moreover, some flexible and abrasive material is easily tied-up in or may wear by the long Bowden tube.

In Fig. 1, a Bowden extruder style machine is used to illustrate the critical components of the 3D printer. The extruder's hot end is the most common location for monitoring and is typically used for gathering information related to nozzle clogging, nozzle temperature, filament melting condition, and nozzle movement. The second most common monitoring position is the cold end. Information related to filament feeding conditions and filament slippage is typically measured here. Thirdly, the heated build platform is used for collecting information about the printing process, including heated build platform temperature and vibration data. In addition to these locations, the filament itself can be monitored to collect filament quality and condition data (e.g., filament diameter variation and filament breakage) at a variety of locations either on or off the printer.

In the section that follows, a discussion of extruder state monitoring, which includes extruder's cold end, hot end, and nozzle state monitoring is presented in Section 2.1. Next, Section 2.2 discusses the state-of-the-art in filament state monitoring relates to filament breakage, filament runout, and filament property monitoring. Lastly, Section 2.3 covers build platform state monitoring.

Table 1
Sensors and methods for the in situ monitoring of the fused filament fabrication process.

Sensors/methods	Printer's health state monitoring	Printing product quality monitoring
Thermocouple	[25–31]	[32–34]
Pressure sensor	[25,35]	
Rheometer	[36,27,29]	
Acoustic emission sensor	[31,37–41]	[37,37,39,42–45]
Vibration sensor	[28,46]	[46]
Accelerometer sensor	[26,35,47–49]	[32,33]
Rotary sensor	[35]	
Temperature and humidity sensor	[35]	
Current sensor	[50]	[51]
Force torque sensor	[52]	
Piezo sensor		[53]
Thermal camera	[26]	[32–34,54–63]
Optical camera	[64,65]	[23,30,48,66–102]
Microscope		[24]
Borescope		[26,28]
Laser scanning		[97,103–110]
Flatbed scanner		[111]
Encoder	[30,112]	
Magnetometer	[35,48]	
Ultrasonic device		[113,114]
Physics-based compressive sensing		[115–117]
Coherent gradient sensing		[118]

2.1. Extruder state monitoring

The extruder component plays the most crucial role in a 3D printer, whose condition directly determines whether the printing is successful. As mentioned above, it includes two parts, the cold end and hot end. The following text is organized as follows: Section 2.1.1 presents the work that has been done on the cold end state monitoring, hot end condition monitoring is described in Section 2.1.2. Section 2.1.3 reports research on nozzle monitoring. Although the nozzle is part of the hot end, its significant impact on the printing process (e.g., layer resolution and printing speed) necessitates a separate section.

2.1.1. Extruder cold end state monitoring

The cold end consists of a stepper motor, hobbed bolt or gear, spring loaded idler to hold the filament, and tubing to guide the filament. In the cold end, the stepper motor drives the filament towards the hot end. The stepper motor is able to impart full torque at low speeds and make small movements at relatively high level of precision. As the cold end module applies the force required to push the filament smoothly through the

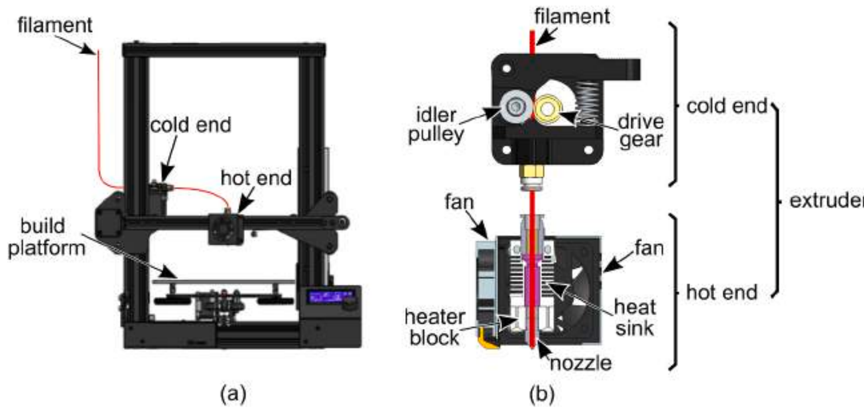

Fig. 1. The profile of the most common consumer-grade 3D printer: (a) the 3D printer's key components; and (b) the layout of the extruder's cold end and hot end.

heat block and nozzle, monitoring the extruder's cold end condition is essential. Most of the fault that occurs on the cold end module are filament transport slippage and abnormal filament feed rate. Also, various research on filament breakage and filament runout are detected at the cold end. For the sake of clarity, these are discussed in Section 2.2.

The most common approach to identifying different cold end states is by analyzing vibration signals obtained from the sensor mounted on the cold end module. Liu et al. demonstrated a method to recognize and classify different extruder states by combining extracted and reduced features from the AE signals with the unsupervised clustering fast search and find of density peaks (CFSFDP) algorithm [37]. This method provides an accurate and reliable real-time system for monitoring the 3D printer's health and can classify the cold end states such as filament loading or unloading and filament runout. Wu et al. proposed a non-intrusive monitoring method by integrating AE sensing technology with support vector machines (SVM) for classification [38]. This method is capable of recognizing three different extruder cold end conditions, which are material loading, normal extruding, and filament runout. Bukkapatnam et al. developed a two degrees of freedom lumped mass model [47]. By extracting the printer's vibration feature with this model, uncommon cold end conditions such as fast feed and slow feed could be identified. Wu et al. developed a more versatile algorithm using a hidden semi-markov model (HSMM) to diagnose the extruder states [40]. This new method reduces the input AE data's dimensions and sizes while achieving more than 90% accuracy with the time resolution of 0.1 s. The experimental result shows that the HSMM algorithm could

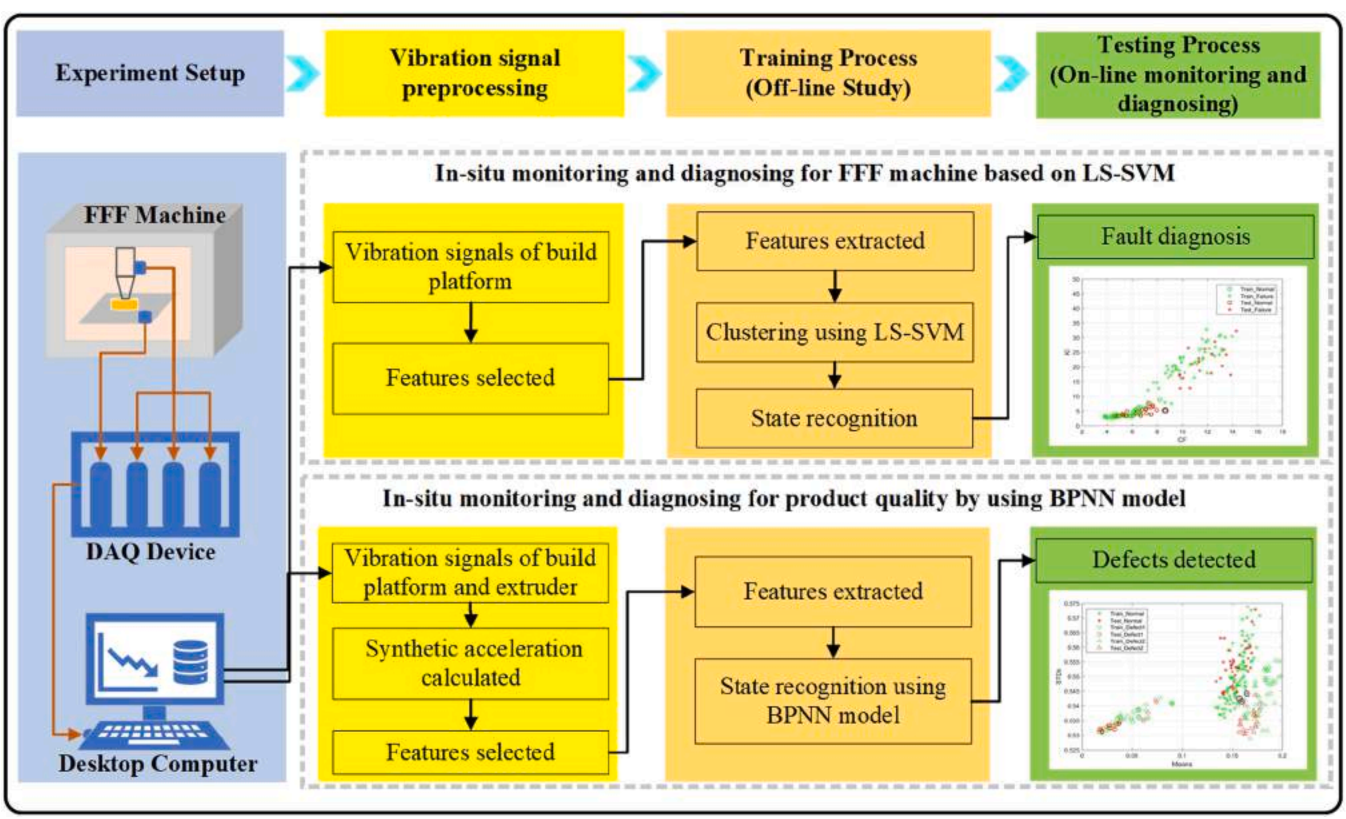

Fig. 2. Flowchart for combined in-situ monitoring and diagnostic of a FFF machine and product quality, showing, (top) the flowchart for in-situ monitoring and diagnosing 3D printer healthy state in the FFF process, which uses the build platform vibration data as input data, after the offline training, the LS-SVM algorithm diagnoses the printer fault online, and (bottom); the flowchart for in-situ monitoring and diagnosing FFF product quality, which utilizes the vibration data from build platform and extruder as input, after the offline training process, the BPNN model detects product defects online [46].

achieve multi-state (filament loading and unloading, filament runout, idle, and normal extruding) identification simultaneously. Furthermore, Li et al. demonstrated that through utilizing a least squares support vector machine (LS-SVM) and combining the vibration data extracted from the extruder and heated build platform, a filament jam state could be effectively recognized with an accuracy of over 90% [46]. Fig. 2 shows in situ monitoring and diagnosing details for the FFF printing process developed by Li et al. [46]. In the flowchart, BPNN is the back-propagation neural network, LS-SVM is the least squares support vector machine, and DAQ is the data acquisition system. By analyzing the vibration signal, the system can diagnose the filament jam failure caused by spring fatigue (i.e. weakening of the spring). Under normal condition, the spring keeps the drive wheel aligned with the cold end filament connector. When the spring fatigues, the drive wheel displaces, thus increasing friction force between the cold end filament connector and the filament.

Accurate knowledge of the filament feed rate is necessary to guarantee product quality during printing. However, filament slippage can occur between filament and feed gear, which leads to product functional and dimensional error. Greeff et al. combined an image processing system with a microscope video camera to explore the speed difference between filament and extruder feed gear speed [65]. The study shows that feed rate and extrusion temperature are the two main factors that influence the slippage rate, but adding closed-loop control to the extruder can decrease the slippage rate considerably. Go et al. explored the slippage rate limits in the FFF printing process [147]. Part of the research shows the relationship between filament shear failure and extrusion force. Fiedler et al. designed a new extruder drive bolt's tooth geometry and evaluated the filament grip force generated from it [21]. A smart FFF 3D printer was built by Moretti et al. with heterogeneous sensing (e.g., camera, thermocouple, positional encoders, and filament encoder) [30]. By mounting an encoder on the back of the drive motor to track the filament advancement, which can indirectly evaluate the extruder material feed rate. This encoder can detect a 7.5 μm minimum filament advance.

2.1.2. Extruder's hot end state monitoring

As hot end conditions directly affect the inter-layer bonding, monitoring the extruder's hot end condition is essential in determining the 3D printer's state [54,148]. Generally, the extruder hot end condition can be divided into three states: normal-extruding, semi-blocked, or completely-blocked. Unhealthy hot end conditions result in reduced product performance such as fatigue, flexural, or strain properties [142, 149,150].

Researchers have demonstrated various successful methods for monitoring extruder hot end condition. One of the common methods used for inferring the hot end conditions is using AE. AE sensors detect the release of acoustic energy caused by the rapid release of localized stress energy in a material (e.g., the polymer being printed). Acoustic events can be caused by a variety of abnormal phenomena. It is sensitive to any of the extruder's hot end states, and as such advanced signal processing techniques must be applied to the acquired data to detect anomalous extruder states. An approach to detect and classify different extruder states by utilizing the features from the AE signals as input data was proposed by Liu et al. [37]. The unsupervised clustering fast search and find of density peaks (CFSFDP) algorithm is trained by the features from the AE signals. This approach is shown to be useful for the real-time monitoring of the 3D printer's health, especially for the extruder's hot end health state. Fig. 3 shows the established extruder condition monitoring platform developed by Liu et al., which consists of an AE sensor, a preamplifier, a data acquisition card, and a desktop computer. A non-intrusive monitoring system was proposed by Wu et al. to classify the extruder hot end states [38]. This approach combines AE sensing technology with the SVM algorithm, which can recognize semi-blocked and blocked hot end conditions.

Another method for monitoring the extruder hot end state is to

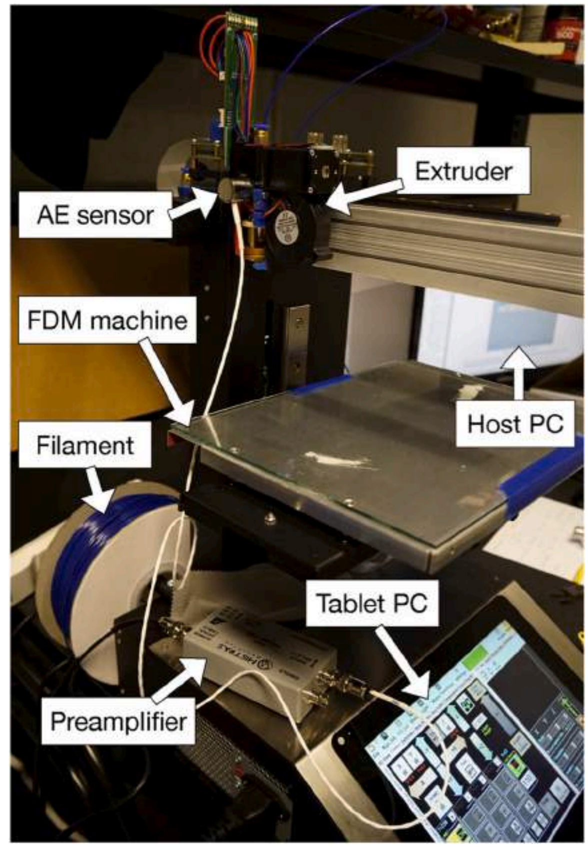

Fig. 3. AE sensor-based condition monitoring platform [37].

monitor the vibration signals by either vibration or acceleration sensors [151]. The model (two degree of freedom lumped mass model) for cold end monitoring by Bukkapatnam et al. [47] was also used to recognize the overflow, underflow, fast feed, and slow feed anomalous conditions for the hot end. Moreover, Rao et al. built an online real-time quality monitoring system using heterogeneous sensors, including accelerometers mounted on the heated build platform and extruder head to measure the vibration [26]. The system could identify the normal state, abnormal state due to insufficient filament extrusion, and failure to extrude state cause by nozzle clog.

Images or videos captured by cameras also have been used to monitor various hot end conditions, such as blockages and missing material flow. Extruder hot end state can be quantified using either a person-in-the-loop, advanced image processing algorithms, or a combination of the two. If the system is automated, it can achieve real-time extruder hot end state monitoring. Rao et al. utilized a borescope fixed on the printer's extruder to get a real-time video of the extrusion process, allowing people to visually monitor the extruder's status during printing [26]. Another real-time monitoring system for advanced manufacturing processes is called the online sparse estimation-based classification proposed by Bastani et al. [28]. By applying the Bayesian estimation method to analyze sensor signals (i.e., thermocouples, vibration sensors, and infrared melt pool temperature sensor), the system can detect the printing process drift (process state change from normal to abnormal and finally completely stops due to the clogged nozzle) with an accuracy of 90% (F1-score). Baumann et al. proposed an auxiliary thresholding algorithm, which can convert digital images captured from the camera fixed on the print-head into binary images to monitor the extruder state [64]. The system can get an accurate distinction between the object and object's background by utilizing this algorithm. Moreover, this system can detect abnormal extruder states such as missing material flow due to a clogged nozzle, air-bubble in the extruder, or jammed material.

Beyond the hot end module, other components also impact product quality, and have invoked the researcher's interest. Fans on the extruder's hot end also play an important role in obtaining excellent product quality, especially the heat sink cooling fan. The heat sink cooling fan is required as it keeps heat from transferring up into the other components. Note that the fans for cooling down the printed layer are optional [24]. To avoid improper fan speed impact on the product quality. Gao et al. utilized acoustic information to predict the fan speed, which could prevent the defects caused by improper fan speed [48]. Kim et al. built a data-driven in situ FFF monitoring and diagnosing system by utilizing an AE sensor and an accelerometer [42]. The author designs a bolt loosening error to drive the nozzle head abnormal motion, which produces interlayer shifting. After the signal processing and feature extraction process, the SVM-based algorithm is used to diagnose whether the printing process is healthy or faulty. The result showed the non-linear SVM-based model had an accuracy better than 87.5%.

2.1.3. Nozzle state monitoring

Variations in nozzle temperature, nozzle distortion, and nozzle clogging can occur in the heated nozzle. Of these, nozzle clogging is one of the most frequent printing errors. Given the persistent challenge of nozzle clogging and its prominent effect on the product's geometrical accuracy and mechanical properties, a majority of research has focused on this area [152]. He et al. proposed an online defect monitoring approach for the FFF process based on the product's temperature field variation [62]. To get the product's layer temperature, an infrared (IR) thermal camera is utilized. After feature extraction, the difference between normal and abnormal printing features are calculated. This proposed approach not only detects the defects but also monitors the nozzle working state. The detection of nozzle blockage can also be monitored by tracking melt pool temperature data. Rao et al. demonstrated that normal, abnormal, and failure process states showed a recognizable pattern by analyzing the melt pool temperature data obtained from the non-contact IR temperature sensor [26]. By applying the nonparametric Bayesian and Dirichlet process mixture model and evidence theory (ET) with this data, this defect detection method can identify the abnormal FFF process such as nozzle clog with high accuracy (85% average F1-score). Some corrective actions can be applied to avoid nozzle clogging by detecting the temperature drift process from normal to abnormal. Nuchitprasitchai et al. built an open-source low-cost real-time monitoring system with a variety of cameras that can detect clogged nozzles, filament runout, or object geometry error using a stereo calibration algorithm [69–71]. Kim et al. studied a methodology to detect material deposition status [51]. The research demonstrates that the nozzle's extrusion pressure affects the current draw from the feed motor, which shows the potential to detect nozzle states using this methodology. A dynamic current-based model was proposed by Tlegenov et al. to monitor nozzle conditions [50]. By modeling the relationship between the current draw, extruding torque, and effective nozzle diameter, nozzle clogging conditions could be identified. This work is validated experimentally by monitoring the extruding stepper motor's current draw with a current-based monitoring system. Moreover, Tlegenov et al. proposed a method to predict the nozzle condition by analyzing the acceleration's amplitudes recorded by an accelerometer fixed on the extruder [49]. The setup used by Tlegenov et al. is shown in Fig. 4. Results from both the theoretical modeling and experimental study verifies that the amplitude of vibration shows a non-linear increase as the nozzle becomes clogged for both direct and Bowden extruders.

Monitoring the filament flow rate and nozzle melting temperature are also commonly carried out for the nozzle conditions. Anderegg et al. developed a method that used pressure transducers and thermocouple insertion devices, so the nozzle temperature and pressure distribution during the printing process can be measured, which gives vital insights for monitoring and improving the printing process [25]. Coogan et al. designed an in-line FFF rheometer by incorporating the pressure transducer and thermocouple into a modified nozzle, which could provide accurate filament viscosity, filament feed rate, as well as melt temperature during the printing process [36]. Balani et al. optimized the FFF printing conditions by exploiting the printing parameters and PLA's physical properties [153]. A series of results are achieved in this research, such as filament's maximum inlet velocity in the liquefier, the PLA's rheological behavior, and the distribution of the velocity along the nozzle radius. Filament flow and temperature history in material extrusion were investigated by Peng et al. [27]. Filament temperature evolution is investigated by embedded thermocouples. Filament flow behavior is achieved by an introduced dye marker within the filament. The experimental results show that the shear rate near the center of the filament is lower, which results in a more blunted velocity profile, and the material extrusion is a highly non-isothermal process. Moreover, Coogan et al. built a model to predict the material extrusion product's interlayer strength, which combines a model to predict interlayer contact with another model for predicting polymer chain diffusion [29]. The in-line rheometer added to the nozzle can directly measure the melt temperature and pressure. The heat transfer analysis is achieved by measuring the critical environmental temperatures using thermocouples. Interlayer contact prediction is based on in-line pressure data, whereas polymer chain diffusion prediction is based on in-line viscosity and temperature measurements. A case study using this model demonstrates applicability for real-time defect detection for material extrusion AM processes.

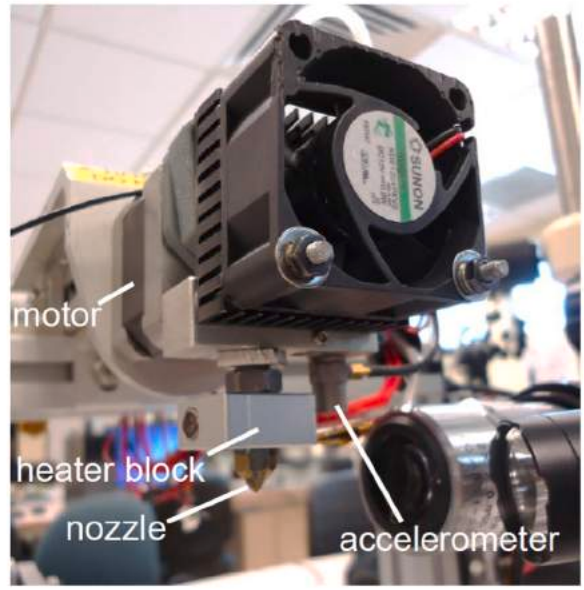

Fig. 4. Accelerometer sensor for detecting nozzle state [49].

Force sensors mounted between the print head and printer frame have also been used to monitor the nozzle's condition, where the printing head and the build platform has a material connection through the melted filament. If the print head's speed is not matched with the extrusion speed, printing defects will occur. De Backer et al. proposed a printing force and torque monitoring solution for the FFF printing process [52]. In this solution, a force-torque sensor is mounted between the printing head and gantry system frame and used for recording and timing the printing force and torque data. By applying an algorithm to the force-torque data, a force and torque intensity geometry map is made. This force and torque intensity geometry map can be used for capturing printing failures by highlighting the product area where the recorded force or torque values are greater than a set threshold. Fig. 5 displays one defect detection sample by using the force and torque intensity geometry map. Fig. 5a shows a twisted decagon product used for

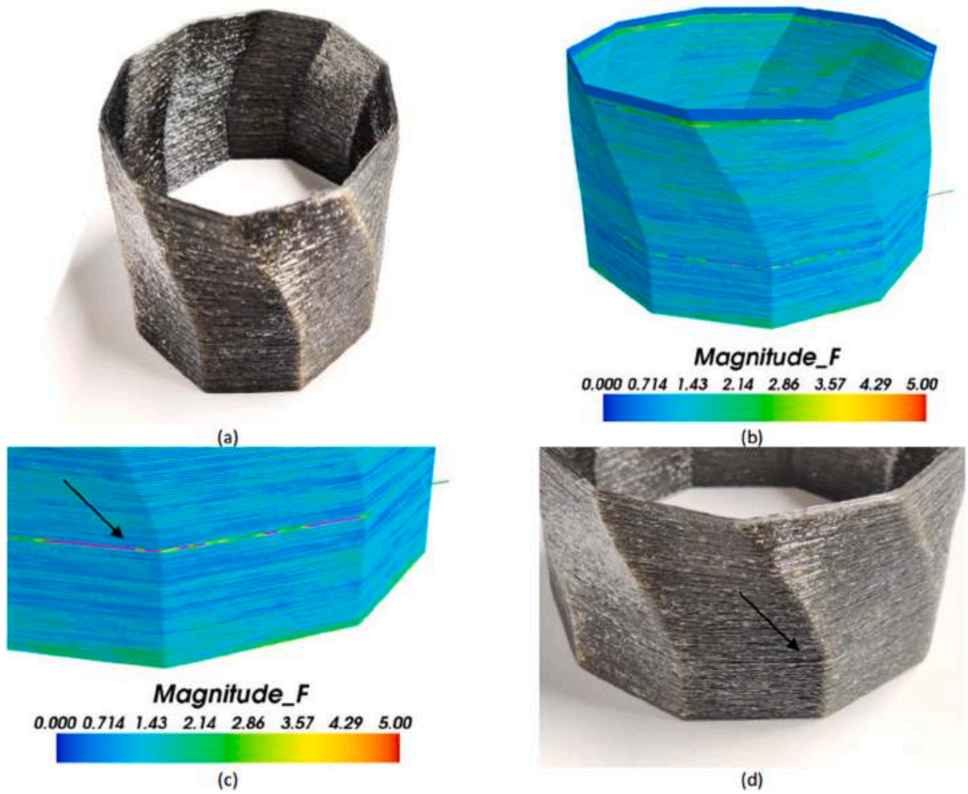

Fig. 5. Twisted decagon sample for defect detection [52]: (a) printed part; (b) the force sensed during the printing; (c) a zone with high measured tension forces; and (d) the resulting defect on the part.

verifying defect detection, and in Fig. 5b is the force and torque intensity geometry map. The detail in Fig. 5c shows an anomaly at the top of the product that is detected by monitoring the force history. As shown in Fig. 5d, the real defect occurs at the same location on the printed product.

2.2. Filament state monitoring

Monitoring filament condition during the printing process helps to guarantee product quality. Consistency in filament parameters such as diameter, moisture, and pigment also have an influence on the final print in terms of product quality and mechanical strength [154,155]. For filament condition monitoring, the majority of research has focused on four cases: filament breakage, filament runout, material classification, and material quality monitoring.

Filament breakage leads to compounding malfunctions such as surface roughness error, geometrical misalignments, or printing failures. Most filament breakage is caused by inhomogeneous filament material, which can not sustain the required pulling force. Yang et al. detected filament breakage with AE sensors, showing that the distribution of the AE signal changed after filament breakage occurred. The signal changes are quantified using two measurable indicators: instantaneous skewness and relative similarity [41]. Between these indicators, the relative similarity is shown to outperform instantaneous skewness. Moreover, the relative similarity is capable of separating the breakage state from the steady state. Fig. 6 shows the AE sensor mounted on the extruder's shell to detect the filament condition. Fig. 7 displays how the amplitude spectrum of AE signals changes under different manufacturing conditions.

Filament runout occurs during printing. Wu et al. developed a method that uses AE hits as an indicator and applies the SVM with the radial basis function kernel to classify the printer running out of filament condition [38]. Liu et al. presented a method to recognize and classify

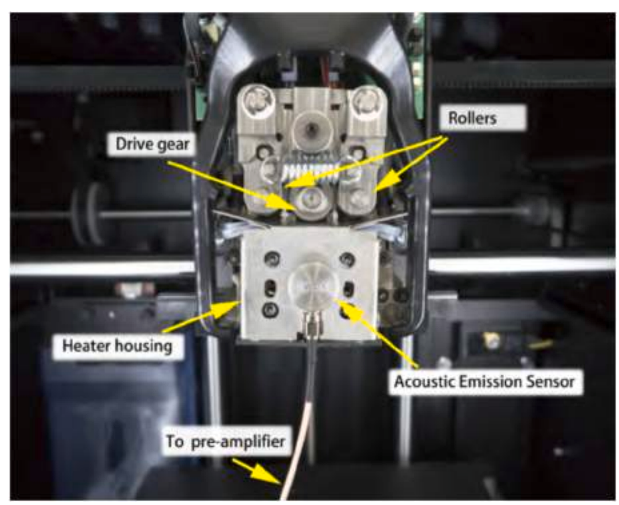

Fig. 6. AE sensor mounts on the extruder shell for detecting filament breakage [41].

different extruder states, including when printer is running out of material, using features extracted from the AE signals [37]. In addition to AE sensors, advanced image processing algorithms are widely used for detecting filament runout. Nuchitprasitchai et al. built a real-time monitoring system with different numbers of cameras by utilizing the stereo calibration algorithm [69–71]. Baumann et al. proposed an auxiliary threshold algorithm to detect filament fault [64]. By converting digital images captured from the camera fixed on the print-head into binary images, this system could detect missing material flow due to filament runout condition.

Filament property varies from type to type, so identifying material

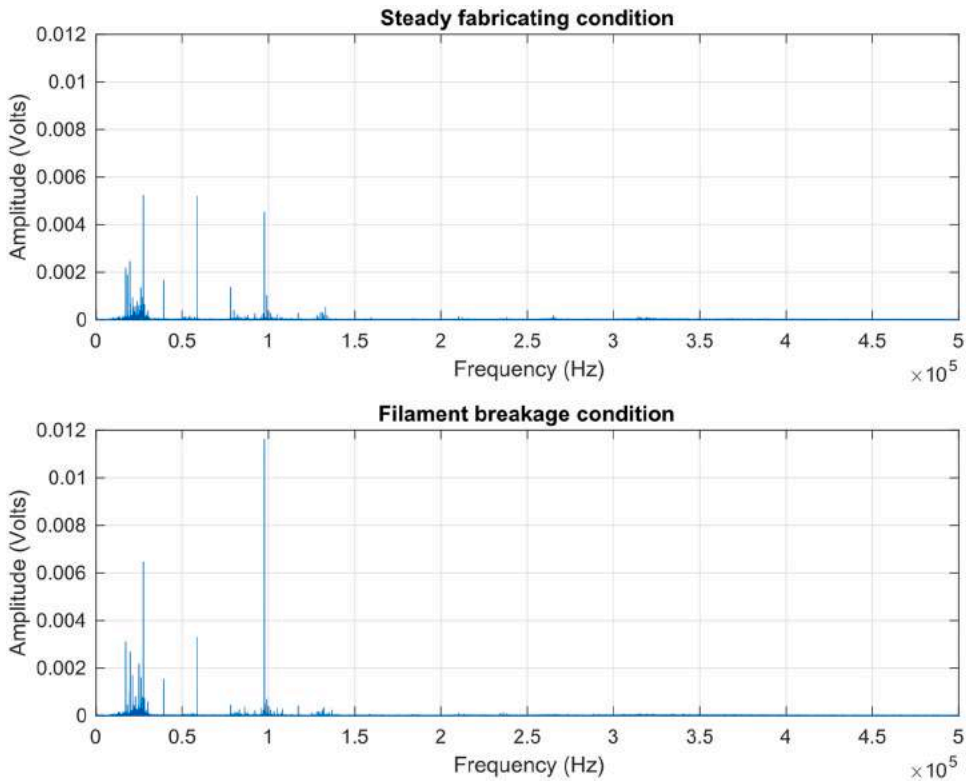

Fig. 7. Amplitude spectrum of AE signals under different manufacturing conditions [41].

properties (e.g., type and color) has also been of interest to researchers from both the print quality and cybersecurity perspective [156,157]. Straub et al. proposed an approach for the filament assurance process, which can compare the filament that is being used with the right one based on the pre-calibration process [82]. The pre-calibration process considers filament type, lighting condition, and other controlling factors compiled by the user and stored in a database. This method can detect the inadvertent loading of incorrect filament and filament contamination during printing.

Polymer filaments with inconsistent diameters will affect final print quality if the variation in diameter is high enough. Inconsistencies in filament diameters may cause slippage, extruder jamming, or bad product quality. Cardona et al. researched the filament diameter tolerances effects in FFF [158]. An array of digital calipers and an optical comparator are utilized to measure the filament diameter. The experimental result indicates that using a low extrusion rate (4.23 mm/s) and moderate extrusion temperature (180 ˚C) combination makes it possible to get high diameter conformity and low diameter tolerance (0.01 mm). Combining mechanical and load cell sensors with different encoders, Soriano Heras et al. developed an advanced filament detection system [112]. The system can detect filament diameter variation and moving conditions while adjusting the extruder's gear speed to match the real printing speed.

2.3. Build platform state monitoring

Monitoring of the heated build platform for undesired temperature variations is essential, as deviations in the temperature of the heated build platform may warp or misalign printing products [159–161]. The two most common parameters considered when monitoring the heated build platform are vibration (by acceleration sensors) and temperature (by thermocouples or IR cameras). To a lesser extent, AE sensors have also been utilized for monitoring the heated build platform state. Li et al. demonstrated that vibration data extracted from the extruder and heated build platform could be used to detect filament jam states with the LS-SVM algorithm [46]. Baumann et al. designed a sensor array including acceleration sensors and thermocouples [35]. Gao et al. built an online process monitoring system to defend against cyber-physical attacks that uses the heated build platform vibration data as one of the indicators to monitor the printing process [48]. Another online real-time quality monitoring system using heterogeneous sensors was developed by Rao et al., which utilizes both thermocouples and accelerometers to monitor the heated build platform [26]. Lastly, Wu et al. combined an AE sensor affixed to the heated build platform with K-means clustering to build a real-time failure monitoring system that could identify the failure time and mode by analyzing the time-domain and frequency-domain AE signal [39].

In the printing process, ensuring that the first layer adheres well to the build platform is the first step in producing a good quality product. However, an unlevel build platform significantly impacts the bonding process and may cause defects such as layer shifting and misalignment. Nam et al. proposed a data-driven approach to diagnosing a mis-leveled build platform [31]. The author uses different sensors, including accelerometers, AE sensors, and thermocouples, to collect the printer's health state information. The flawed process designed in this experiment is the build platform leveling fault, which results in a warpage and bad adhesion. The result verified that the non-linear SVM-based model with the printer frame acceleration root mean square information has the best testing accuracy.

3. Monitoring and analysis of the product quality in the printing process

Monitoring and analyzing the printing process is an enabling technology for real-time quality control as it can diagnose printing abnormalities and defects. In addition to monitoring 3D printer health condition, another main task of a monitoring system is the analysis of product quality. A variety of aspects influence the FFF product quality, including surface roughness, printing infill defects, and dimension or geometry accuracy [162,163]. To achieve the objective of monitoring the printing process and product quality, researchers have proposed various methods that will be discussed in Section 3. Section 3.1 describes the monitoring of temperature variations during the printing process. In Section 3.2, a discussion of in-process printing abnormality is presented, while product surface roughness defects detection is discussed in Section 3.3. Finally, infill defect detection (Section 3.4) and product geometry error detection (Section 3.5) are also presented and discussed.

3.1. In-process printing temperature variations monitoring

As the FFF process deposits individual tracks to form layers, it is critical to maintain thermal energy to ensure there is proper inter-layer bonding [148,164]. When the thermoplastic filament is being extruded from the nozzle's hot end, it is melted and sticky, allowing the material to fuse with the tracks and layers previously deposited on the build platform [165,166]. However, this bonding mechanism is no longer present once the filament temperature falls below the glass transition point. As expected, the lack of inter-layer bonding can affect part performance and geometrical accuracy [167,168]. Therefore, monitoring product temperature during the printing process is being actively investigated as a means to ensure the quality of printed components.

Monitoring the temperature during deposition is important in understanding the filament weld formation. Seppala and Migler utilized IR imaging to measure the polymer's surface temperature profile in the printing process [60]. The crucially important weld temperature temporal profile can be obtained from the printed layer and sublayers temperature profiles. The result shows that the weld temperature drops at a rate of approximately 100 °C/s, with temperature staying above the glass transition for approximately 1 s under typical printing conditions. To quantify the inter-layer weld strength from the polymer inter-diffusion perspective, Seppala et al. built an experimental framework comprising thermography, rheology, and fracture mechanics [61]. They also developed an equivalent isothermal weld time which was then tested in relationship to the fracture energy. Costa et al. illustrated an analytical solution to the transient heat conduction during the filament deposition process [54]. The analysis process is coupled with an algorithm that can activate the related boundary condition taking into account the deposition sequence. The analysis can predict the temperature and adhesion with time evolution by considering the main printing process parameters. The experimental result validates that the analysis prediction agrees with the measurement for both temperature and adhesion.

IR cameras are the most commonly used method for monitoring the temperature of 3D printed components [169]. Dinwiddie et al. used an IR camera set up on a FFF printer to get layer-by-layer thermography images of ABS filament printing process, its thermal behavior and thermal evolution [170]. Malekipour et al. researched an ABS product's layer temperature distribution and average temperature condition by combining the layer-based temperature profile plot with the temporal temperature plot [57]. An IR-based system capable of capturing spatial and temporal temperature variations during the progressive printing process was presented by Ferraris et al. [55]. Li et al. developed a new framework by combining physics-based and data-driven methods to predict the component-scale layer-to-layer thermal field [56]. Fig. 8 shows a temperature variation monitoring system proposed by Ferraris et al. with an IR camera facing the 3D printer's nozzle [55]. The system captured the printing temperature variation from the product's front $x-z$ plane.

Physics-based compressive sensing (PBCS) technology can be used to obtain high-fidelity information by using low-fidelity measurements.

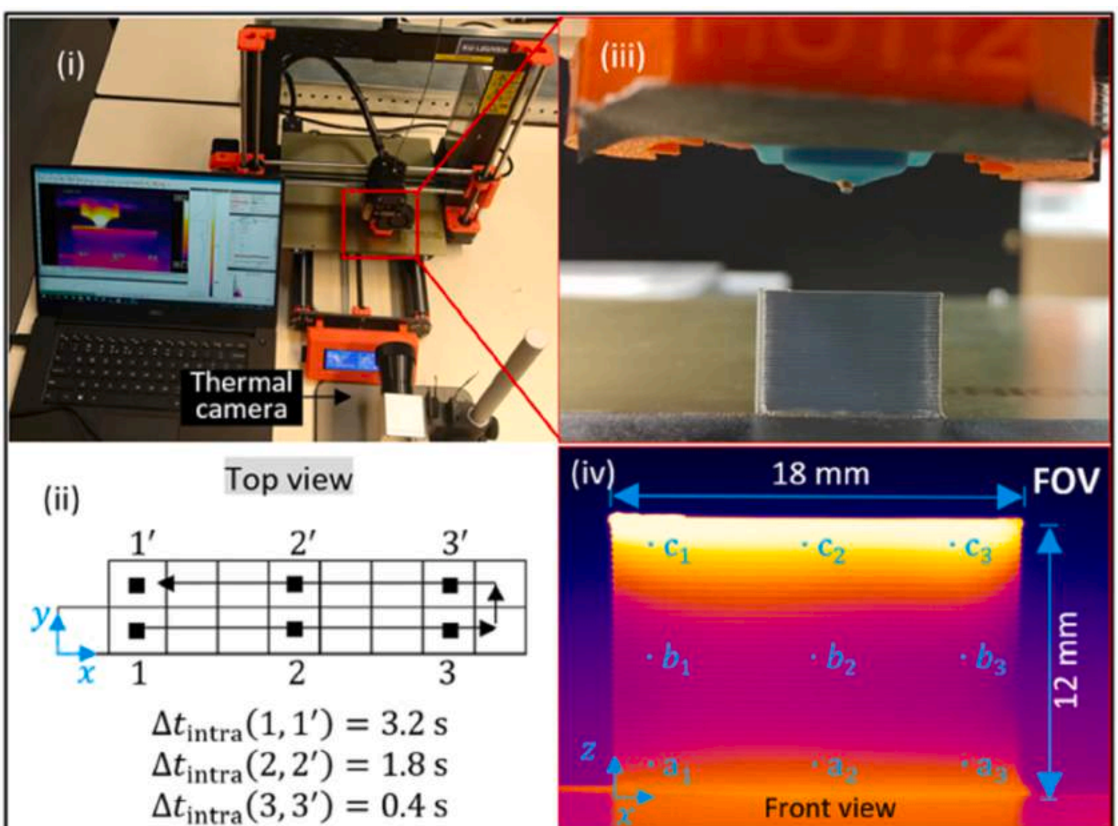

Fig. 8. IR camera for monitoring the printing product temperature [55]: (i) picture of the thermal camera set-up for FFF printing process monitoring; (ii) the product geometry, filament deposition sequence, and intra-layer time for elements located on given x-y planes from the top view; (iii) picture of the printed product; and (iv) thermogram of the printed part.

This technology has also been applied to measure temperature distribution. Lu et al. proposed a new compressive sensing method by applying a physics-based approach to efficiently and precisely monitor the printing process temperature distribution [115]. The PBCS accuracy is assessed by comparing the reconstructed temperature distribution using grayscale thermal images obtained from an IR camera with the temperature distribution getting from the PBCS. This proposed physics-based compressive sensing method has great potential to improve monitoring accuracy and efficiency with lower costs by reducing the number of sensors used in the monitoring system. Furthermore, Lu and Wang proposed an efficient transient temperature distribution monitoring approach for the FFF process by using PBCS [116,117]. The printing process can be monitored by reconstructing 3D temperature distributions using the sparse samplings in temporal and spatial domains.

3.2. In-process printing abnormalities detection

The term "abnormal printing process" refers to conditions where the printer is in a perceived healthy condition, but printing failures still occur. These abnormalities include poor bonding quality between the filament and build platform or inter-layers, shrinkage and warpage, and product position error. All these abnormalities have a direct or indirect effect on the printing product quality.

3.2.1. First layer bonding error detection

Poor bonding quality between the first layer and build platform leads to the material peeling off from the build platform, resulting in mechanical contact (i.e., scratching) between the nozzle and distorted material [171]. These failures directly influence the quality of printing parts. The normal and abnormal printing processes are shown in Fig. 9 [39]. To expand, Fig. 9a shows a normal printing process where the material is deposited by the nozzle smoothly and the filament is correctly attached to the heated build platform. A failed process is shown in Fig. 9b, where the filament does not adhere to the heated build platform.

Various sensors have been shown to be capable of detecting abnormal bonding processes such as filament peeling and dragging. Wu et al. set up an AE system attached to the upper surface of the heated build platform [39]. AE events vary significantly when the material is peeling, warping, or dragged by the nozzle as compared to the normal printing process. The research result shows that abnormal printing failures could be automatically identified by K-mean clustering. Wu et al. proposed an online data-driven monitoring approach based on the AE sensor for the FFF process to diagnose the process failure [45]. An unsupervised ML algorithm self-organizing map (SOM) is utilized to cluster different failure modes. The proposed method could detect three types of failure: scratching and hitting between the distorted filament and extruder, filament peeling off from the build platform, and material rubbing by nozzle or gliding on the build platform. Bhavsar et al. presented a methodology to detect first layer bond quality for the FFF printing process by utilizing piezoelectric sensor and the discrete wavelet energy approach [53]. The research shows that the first layer's good or bad bond quality can be detected by analyzing the piezoelectric polyvinylidene difluoride sensor's vibroacoustic signals.

3.2.2. Inter-layer bonding error detection

The interfacial bonding quality has a significant impact on the product's mechanical property. Delamination is a printing failure, which is usually caused by improper fusion between the previous layer and the new layer. While it is a local defect, it can affect the entire printed product.

Researchers have developed various approaches for delamination detection. Jin et al. built an automated real-time interlayer defect detection and prediction system for the FFF process. By combining real-time camera images with the CNN algorithm, this system is able to detect delamination, which is caused by the improper spacing between nozzle and build platform. Accuracy on validation data is 97.8%, shown in Fig. 10 [94]. In Fig. 10a, a camera connected over USB is mounted on the left side of the nozzle to capture the printing images. Fig. 10b shows product quality images for four different representing four nozzle spacing conditions. The "High" in Fig. 10b means the nozzle height between the filament and build platform is high, which leads to poor adhesion quality. Furthermore, a "High+" nozzle height makes the delamination even worse. On the other hand, the "Low" nozzle height results in a nonuniform surface quality due to the restricted space under the nozzle. Cummings et al. presented an in-process ultrasonic inspection for AM product [113]. Four piezoelectric transducers are bonded on the build platform to inspect the product periodically in the printing process. By comparing the normalized frequency response with the experimentally determined ideal response, the system can find defects such as delamination in recently printed layers.

Other methods have also been explored for monitoring and assessing the interlayer bonding quality. Xu et al. presented a real-time AM process monitoring system by applying phononic crystal artifacts [114]. This research is based on ultrasonic wave propagation in phononic coupons consisting of repeating substructures, which can be used to monitor and finally assess product bonding quality and uniformity. Product structure periodicity results in the dispersion of the wave, which is easily affected by geometric or materials properties and irregularities. To predict the filament connection quality between lines in different printing parameters, Jiang et al. proposed a deep learning ML model to predict the filament bonding quality for the FFF process [172]. Filament extrusion speed, print speed, layer height, and line distance are chosen

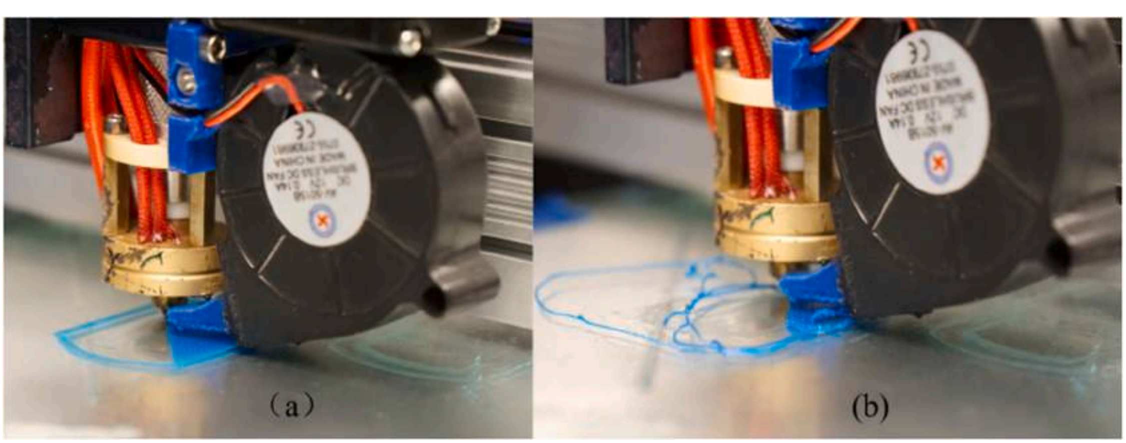

Fig. 9. Image of normal and abnormal printing process [39]: (a) normal FFF printing status; and (b) abnormal FFF printing status.

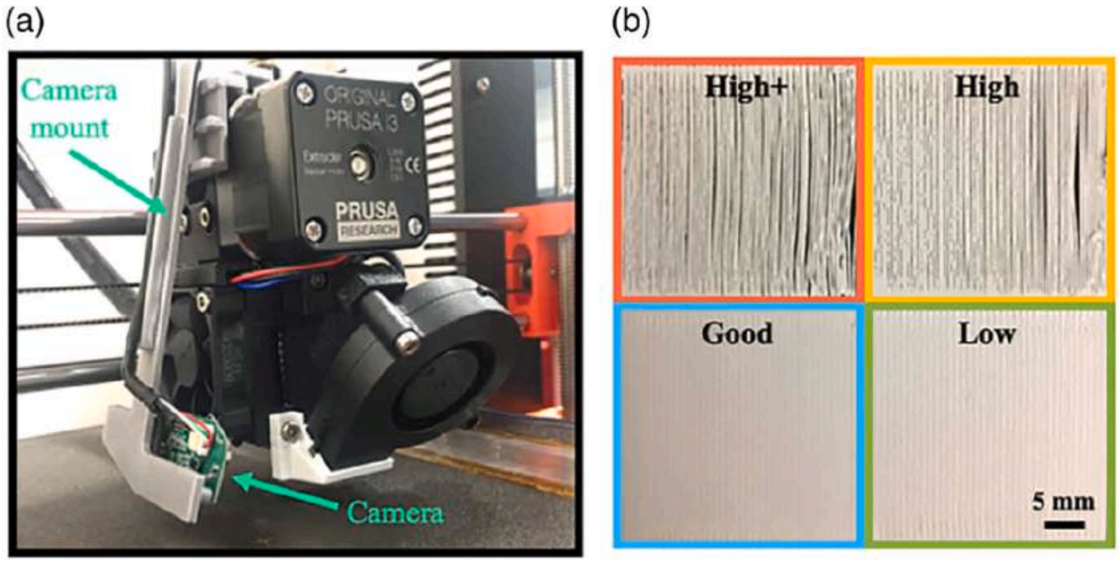

Fig. 10. Delamination detection system setup and product quality images: (a) the monitoring system with a camera mounted on the extruder; and (b) four cases product quality images, which represent the four nozzle height condition [94].

as the deep neural network's input, and the layer connection quality is the output. The prediction accuracy of this ML model can be as high as 83%.

3.2.3. Shrinkage and warpage error detection

Detecting shrinkage and warpage in the printing process is important to control the geometry tolerance. During the printing process, when the printed polymer cools down, its volume decreases, even though its temperature is still above the glass transition temperature. When polymeric parts cool at different speeds or in an anisotropic way at diverse positions, the printed product is prone to warpage [173]. As a common printing error, detecting product shrinkage and warpage are essential to getting a good printing product.

Researchers have investigated the relationship between warpage and printing parameter settings. Panda et al. built a warp performance evaluation model to evaluate the process's warping characteristics [171]. The proposed evolutionary system identification (SI) method quantifies the warping by the printing process parameters, including line width compensation, extrusion velocity, filling velocity, and layer thickness. Analysis results show the layer thickness and extrusion velocity affects warping the most. To study how the printing process variables affect the product warpage in FFF, Armillotta et al. selected three variables related to product's geometry (i.e., length, width, and height) and the layer thickness as influence factors [174]. The research identifies the influence factors individual and interaction effects on the warpage generation.

A series of shrinkage and warpage detection methods have been introduced by researchers. Hu et al. illustrated a FFF printing fault detection method, which explores the classification of faults produced by the temperature filed variation [63]. With the SVM algorithm, the method can recognize different defects (i.e., insufficient filling, warping, and serious fault printing). Saluja et al. built a closed-loop FFF in-process warping detection system [98]. They extract product corner features as input into the CNN model, while the probability of a product corner being warped is output. The experimental result shows the mean accuracy yield from this model to be 99.3%. Fig. 11 shows the process proposed by Saluja et al. to detect the warpage for the FFF printing process [98]. Li et al. proposed a product status recognition method for the FFF process by utilizing the AE sensor [43]. Two algorithms, HSMM and SVM, are applied to recognize the product normal, looseness, and curl status. The result shows the HSMM performs a bit better than the SVM. Jin et al. built an automated real-time interlayer defect detection and prediction system for the FFF process [94]. By fixing a strain gauge on the build platform, this system could detect product warping. Li et al. demonstrated that by utilizing a back-propagation neural network (BPNN) and combining acceleration data and vibration data extracted from the extruder and heated build platform, warpage product defects and abnormal filament leakage could be detected [46]. The result shows the diagnosis accuracy by BPNN is over 95%.

3.2.4. Product positioning error detection

Product position discrepancy influences product quality. Straub et al. developed an identification and decision-making system integrated with quality control process for identifying the object position discrepancy [78]. The system can compare the object's silhouette taken from CAD files with actual product positions to identify the matching extent. Baumann et al. developed a vision-based error detection system [64]. The system uses cameras to obtain the printing process video and then applies the developed image processing algorithm to analyze them. As the normal printing product only grows vertically, a suddenly increasing

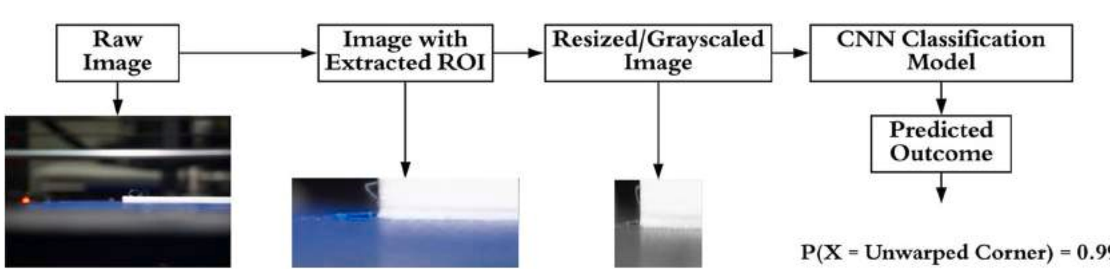

Fig. 11. Image acquisition and analysis pipeline for the warpage classification [98].

horizontal pixel indicates horizontal movement (i.e., product detachment from the heated build platform). The algorithm achieves detachment detection by calculating image differentiation between two consecutive images. Results show that the system could detect product detachment in a short response time. By integrating multiple heterogeneous sensors, a smart FFF 3D printer was built by Moretti et al., to monitor the printing process and product quality [30]. The nozzle path can be reconstructed by the X, Y, Z position information from the exes positional encoders. The positioning error resulting in a visible misalignment can be detected by comparing the measured nozzle path with the nominal G-code path.

3.3. Product surface roughness quality monitoring

Surface roughness is a significant factor in part quality as it influences critical product precision, especially its functionality or assembly at mechanical interfaces [175]. When the extruder is in an under-extrusion or over-extrusion condition, product surface roughness changes drastically during the printing process [61,58,176]. Guaranteeing that the product's surface roughness is within specifications is a critical part of the FFF printing process. Discussion will focus on both the data-driven and model-based approaches.

3.3.1. Data-driven product surface roughness quality monitoring

Data-driven approaches to monitoring product surface roughness errors have been developed. In the development of these purely data-driven methods, most of the research studies use cameras to get real-time images or video and then apply advanced algorithms to process the images and identify the product surface roughness condition.

ML algorithms are commonly utilized by researchers to detect product surface roughness. Jin et al. mounted a camera on the FFF printer [68], as shown in Fig. 12a. Different product qualities for under-extrusion, good-quality, and over-extrusion conditions are shown in Fig. 12b. These images are used to build a pre-trained data set, which is trained by a ResNet 50 architecture CNN classification algorithm. After that, real-time monitoring and refining is implemented, by feeding real-time images into the pre-trained classification mode, the current condition can be obtained. Liu et al. designed a system for defect recognition that uses the texture analysis-based image diagnosis (TA-ID) algorithm to process surface images taken by a digital microscope [24]. The system can recognize the effects when in conjunction with a supervised classification algorithm. The system could even adjust the related printing parameters (i.e., cooling fan on/off and material flow rate) to mitigate printing defects online through closed-loop feedback control. Wang et al. developed a vision-based online monitoring system to identify surface defects [99]. In this system, a mobile camera system is designed to monitor the product's exterior surface from different angles. By utilizing a CNN algorithm, this system can detect the blob, void, thick line, crack, and misalignment defects. Moreover, Banadaki et al. built a reliable real-time quality monitoring system with a DCNN algorithm [90]. After training the model on images taken at each layer, the proposed online model can classify five different quality grades resulting from overfilled or underfilled with an average accuracy of 94%.

Other data-driven approaches utilize various advanced algorithms that could also achieve product surface quality assessment by analyzing the product texture images. Huang et al. proposed a statistical process monitoring (SPM) approach based on image data from a optical camera [93]. As the images' mean intensity values change when the printing process is in different states (e.g., overfill and underfill), the monitoring for the manufacturing process can be achieved by calculating the generalized likelihood ratio (GLR) statistics for each image's determination of regions of interest (ROI). The case study shows the proposed approach is effective in monitoring surface roughness for the FFF printing process. A series of methods were proposed by Okarma and Fastowicz et al. for assessing printing product surface quality. For example, an approach that investigates the product quality based on a gray-level co-occurrence matrix (GLCM) and Haralick features to analyze printing images for texture analysis was proposed by them [76]. This quality assessment method could lead to satisfactory surface distortion detecting and promising future deployment into the 3D printing process. A full reference image quality metric for assessing 3D printed product surface roughness was designed by Okarma et al. It uses printing process images captured by a camera and could achieve a classification accuracy of 96.8% [74]. Another method is color independent product surface quality assessment based on image entropy, which can be applied for 3D printing monitoring as well as the product quality inspection without considering the filament color [77]. An improved color surface quality assessment approach based on image entropy was proposed recently by Okarma and Fastowicz [85]. With less than 100 samples, this color-independent quality assessment approach can identify the high or low surface quality. Beyond the approaches mentioned above, other quality assessment approaches were introduced by Fastowicz et al. The first approach uses Hough transform and histogram equalization, which has a very promising classification accuracy, especially for the scanned images [80]. The second approach is an automatic product surface quality assessment based on the entropy of depth map images [79]. By equipping the fringe pattern-based 3D scanner on the 3D printer to get the most helpful product surface images, this approach's classification accuracy can exceed 90%, with the F1-score over 92%. As the authors have published a series of related papers about surface quality assessment, the remaining papers are listed here for the convenience of the reader [75,84,86–89].

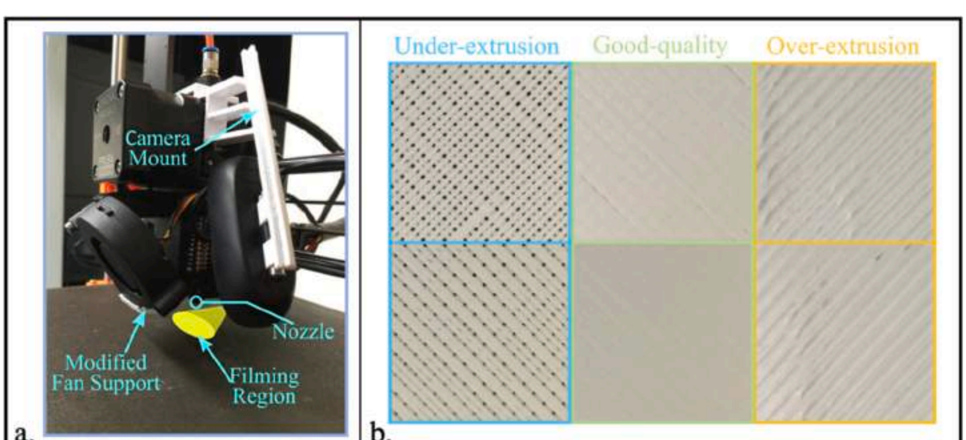

Fig. 12. The experimental setup and product quality under different extrusion conditions: (a) camera setup on the 3D printer; and (b) representative images for 3D-printed blocks under different printing qualities categories of under-extrusion, good-quality, and over-extrusion [68].

3.3.2. Model-based product surface roughness quality monitoring

In addition to the data-driven approaches discussed above, different model-based approaches have been developed, including the utilization of CAD model to detect and quantify the surface roughness, models to understand the printing parameters effect on surface roughness, and surface roughness prediction models.

Precision CAD model is a common component that is used to assess the surface roughness quality. These CAD model-based methods often utilize advanced algorithms in combination with models to detect and quantify product surface roughness. Sohnius et al., proposed a method which can predict the location of surface defects [110]. For this method, two 2D laser profilometers are mounted on the 3D printer's extruder to record the point cloud's surface profile. By comparing the target model path (taken from the CAD model) with the actual path (produce from the point cloud), the surface defects can be detected. In this research, three ML algorithms (random forest, decision tree, and artificial neural network) are utilized. The result shows that the classification accuracy for the gap defect is over 95%. Cheng et al. built a closed-loop online process control model for increasing the product surface quality [23]. In their system, 3D surface reconstruction is achieved by intensity images obtained from a CCD camera based on the CAD model. By applying a 3D reconstruction surface with a machine vision (MV) process feedback system, the filament flow rate could be adjusted to reduce the over-extrusion or under-extrusion defect. Hurd et al. developed a quality assurance for the AM process using mobile computing [83]. The system has four parts: (1) 3D printer, (2) a host computer that controls the 3D printer with G-code, (3) a mobile device to achieve the visual quality assurance, and (4) a server that supplies communication between the mobile device and host computer. Two image processing algorithms (i.e., image subtraction and image searching) are used to detect filament misprint by comparing the printing layer's image with the reference image from the 3D model. The proposed system can detect printing errors and determine whether the printing should be stopped.

Printing process parameters have been studied to quantify their effects on surface roughness. Jin et al. developed a new surface profile quantitative analysis model for the FFF product [177]. The printing process parameters (i.e., layer thickness and stratification angle) and fabrication process parameters (ratio between flow rate and feed rate) are the two groups used for examining their effects on the surface quality. The experimental result verifies the proposed model is feasible and effective on surface quality enhancement by optimizing the printing process parameters. Chaidas et al. investigated the temperature changing effect on the surface roughness [178]. The result shows that with the temperature increasing, the product surface roughness decreased. Akande et al. tried to find the optimum printing parameters to manufacture products with good surface quality and dimension accuracy [179]. Layer thickness, printing speed, and fill density are chosen as printing factors. The experimental results show that layer thickness is the most significant printing parameter for both surface roughness and dimension accuracy. Galantucci et al. carried out the research about the tip size, raster width, and slice height, three parameters that have an effect on product surface roughness [19]. The results verify that the slice height and raster width has a more significant impact on surface roughness.

The surface roughness prediction model based on printing parameters is also a research hotspot, as various prediction models have been developed. Ahn et al. put forward an approach to formulate the FFF product surface roughness, which is based on the main printing parameters (surface angle, layer thickness, cross-sectional shape of the filament, and overlap interval). The research investigates the effects of printing parameters on the product surface quality [180]. Comparing the result between the real surface data with the estimated values shows the proposed model can get elaborate surface roughness predictions. Kaji et al. proposed a methodology to predict the final product surface roughness quality, which is based on the layer thickness and local surface slope [181]. A data-driven product surface quality predictive model for the FFF process was proposed by Li et al. [32,33]. The author chooses extruder temperature, layer thickness, and print speed ratio to extrusion rate as input data to understand the effect of the printing parameters on surface roughness. After the feature extraction process, a random forest algorithm is utilized to predict the surface roughness. Dambatta et al. built an adaptive neuro-fuzzy inference system (ANFIS) model to predict the surface roughness for FFF parts [182]. Layer thickness, deposition orientation, and geometry are chosen as the input data, the surface roughness is the output. The ANFIS model shows a 93.34% surface roughness prediction accuracy for a fabricated prototype. Vahabli et al. built a hybrid model to estimate surface roughness distribution [183]. The layer thickness and deposition are chosen as input, while the response variable is arithmetic mean surface roughness. The proposed model is demonstrated on various printing samples, and the result shows that the hybrid model can enhance prediction accuracy compared to the previous models. Vahabli et al. raised a new methodology for estimating the surface roughness based on radial basis function neural networks (RBFNNs) [184]. In this research, the input data is layer thickness and build angle; output is the arithmetic mean surface roughness. After optimizing the RBFNNs model by the imperialist competitive algorithm (ICA), the optimized model can get a surface roughness estimation of 3.64% mean absolute percentage error and 2.27% mean squared error.

To reduce surface roughness predictive errors in FFF, Taufik et al. proposed an innovative method to analyze and estimate the randomness in the build edge profiles' geometry [175]. The research result shows that the proposed method can reduce the surface roughness prediction error compared to the existed methods. Barrios et al. compared three different algorithms' (i.e., J48 algorithm, random tree, and random forest) surface roughness prediction performance in FFF [185]. The training data is the samples printed with five different factors (layer height, temperature, print speed, print acceleration, and flow rate) and three distinct levels. The results show that the random tree performs best in this case of study, with an 80% accuracy for the surface roughness in the direction parallel to the direction of extrusion and 86.67% for the surface roughness direction perpendicular to the direction of extrusion. Angelo et al. verified that to get an accurate surface error, it is not adequate to use just the roughness parameters [186]. Angelo et al. proposed a better index, the parameter P_a (ISO 4287 [187]), for evaluating product surface quality and a new model to predict P_a for the product surface roughness manufactured by the FFF process. The new model prediction result shows a good match with the empirical values.

A series of surface roughness prediction methods were put forward by Boschetto et al. for the FFF process. A feed-forward neural network surface roughness predictive approach was proposed [166]. The layer thickness and deposition angle are chosen as input data. After being fully trained, this method can predict the average roughness, matching the actual data very well. A methodology that integrates the surface quality prediction and process design was built by Boschetto et al. [188]. Using layer thickness and printing angle as input, this method can estimate the product dimension accuracy and average roughness. Since the product average roughness is not able to reflect the real surface roughness, Boschetto et al. proposed a novel 3D roughness profile model to extend the characterization to all roughness related parameters by a profilometric analysis [189]. The method can predict a whole surface characterization for the FFF process. Another model was built by Boschetto et al. to examine the coupled operations of barrel finishing and FFF [190]. The built model can predict the surface roughness by using printing process parameters (layer thickness and deposition angle) with the material quantity removed by barrel finishing.

In summary, these model-based approaches emphasize the important roles of artificial intelligence-based image processing and use of data-driven process parameters in the determination of surface roughness of FFF processes.

3.4. Product infill printing defect detection

In contrast to the surface faults and defects discussed in the prior sections, the detection of defects in product infill is especially hard as once the part is completed, detecting internal faults is challenging. Due to the thin nature of the build-up on infill, often only one track wide, improper parameters setting (e.g., extruder temperature and printing speed) can cause faults in the infill affecting the exterior where more tracks help to compensate for small variations in printing. Furthermore, infill is especially vulnerable to cyber-attacks as an attacker could alter the infill in such a way to compromise the part that would be nearly impossible to detect once the part is fully completed [191,192].

Monitoring of infill quality has been highlighted as a potential method for defending FFF from cyber-attacks [192]. Wu et al. presented an approach to detect malicious infill defects of the 3D printing process using a classification-based ML method to analyze the printing process images from the camera [73,193]. With a naive Bayes classifier, an infill defects prediction accuracy of 85.26% could be achieved. Furthermore, if J48 decision trees are utilized instead of naive Bayes classifiers, 95.51% prediction accuracy could be achieved. Fig. 13 shows five different designed infill defect patterns: seam, irregular polygon, circle, rectangle, and triangle defects with 10% honeycomb infill, which almost cover the common infill defect patterns. Gao et al. built an online 3D printer monitoring system for defending against cyber-physical attacks where infill path attack is one of the monitored aspects [48]. The extruder's movement is tracked by using magnetometers to detect magnetic field intensity. The system matches the expected infill path with the measured infill. The average Hausdorff distance (Hausdorff distance describes the largest distance between sample points in two curves [194]) is obtained to quantify error. For 50 layers with different infill rates (from 5% to 20%), the measured error is less than 1 mm. Results show that this system could be used for monitoring the printing infill path error by comparing the extruder's movement path with the designed infill path. By integrating multiple heterogeneous sensors, a smart FFF 3D printer was built by Moretti et al., capable of monitoring the printing process and product quality [30]. With the camera's help, the poor cohesion defect between the infill and the outer wall can be detected from the layer image.

As different infill level impacts the printing product's structural integrity, the product's infill level condition was also studied. Straud et al. used visible light imagery to assess the quality and sufficiency of 3D printing product infill quantity [195]. According to the assessment result by the visible light imagery-based assessment method, this technique can determine if the product's current infill level is appropriate or not.

3.5. Product geometry error detection

A product's geometry accuracy is easily affected by printing process errors such as nozzle clogging, improper build platform temperature setting, or bad leveling calibration. These unanticipated anomalies influence either directly or indirectly product quality, which may produce defects such as product geometry deviation or deformation [196,197]. For these reasons, an in situ monitoring and detection system for product geometry defaults is worthwhile to avoid wasted energy, time, and material [162,163]. Discussion about the product geometry error detection also divides into data-driven and model-based approaches.

3.5.1. Data-driven product geometry error detection

To detect product geometry error, different data-driven approaches have been studied. In these studies, ML algorithms are often used to analyze real-time images or videos to monitor product geometry conditions. An automated geometry defect detection approach was developed by Narayanan et al. [121]. This approach could classify good and defective polymer products manufactured using the FFF process by analyzing the printing product geometry images. Two independent ML methods are implemented to detect geometry defects. First, the principal component analysis (PCA) is utilized to reduce the images' dimension, and then an SVM algorithm is used to classify the product as good or defective, thus achieving an overall accuracy of 98.2%. Next, a deep-learning approach that utilizes a convolutional neural network (CNN) is investigated. This method achieves a 99.5% classification accuracy. Delli et al. built a real-time 3D printing monitoring system by integrating image processing with supervised machine learning [67]. The system is capable of detecting unintended failures such as filament runout or abnormal stop and can detect product geometrical defects during the printing process. Zhang et al. utilized a CNN algorithm to detect unfinished printing failure for the material extrusion 3D printing process [102]. The overall average accuracy in this approach is 70%.

Other non-ML approaches also show good potential for detecting product geometry errors. Yi et al. proposed a defect detection method for the FFF process, which combines the statistical process control (SPC) with machine vision [100,101]. Utilizing SPC to analyze the extracted contour data from the printing process images captured by the camera, the contour profile defect can be detected. The result shows that the monitoring accuracy is 0.5 mm. A zero-defect AM process was developed by Faes et al. [105]. By implementing a closed feedback loop with sensors and a laser triangulation system, the developed algorithm can detect the deposited tracks and identify the z-direction geometrical error when the track is lower than one layer thickness. Li et al. applied a coherent gradient sensing (CGS) system to achieve the in situ deformation monitoring [118]. CGS technology is a full-field, lateral shearing interferometric method, with some advantages, such as real-time, full-field, intuitive, and vibration resistant. Moreover, this method can potentially be utilized in stress analysis for the 3D printing product. The study evaluates the deformation in three different cooling processes (i.e., fast cooling stage, transitional cooling stage, and slow cooling stage). Li et al. proposed a distortion defect diagnosis by utilizing the AE sensor to get the build platform's vibration data [44]. After filtering out the noise from the feature extraction process, this method shows promise for distortion detection; however, determining accuracy needs further study.

3.5.2. Model-based product geometry error detection

Model-based approaches are a common method for product geometry error detection. Significant research has been done to build models for evaluating product geometry conditions. Methods used include those based on CAD and point cloud models. These methods seek to improve

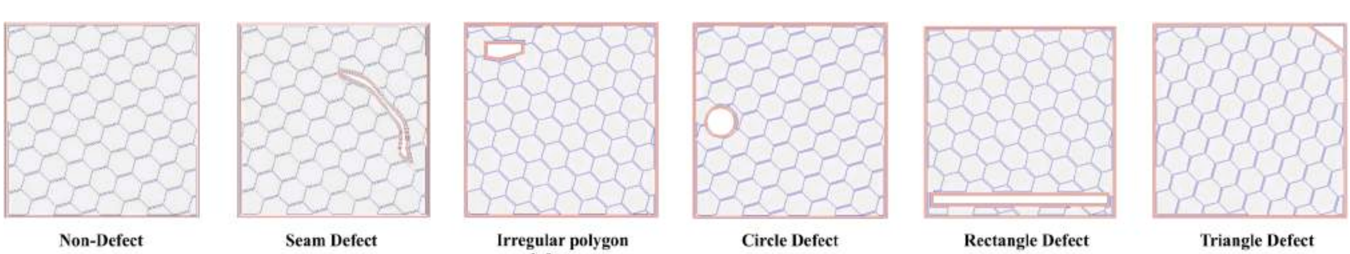

Fig. 13. Types of designed infill defect patterns [73].

and to predict product geometry conditions.

CAD models are one of the most widely used methods to detect product geometrical defects. By comparing the in-process product image with the final product image (e.g., 3-D reconstruction product images and CAD model image), the variations in geometry can be detected. Using cameras for "profile monitoring" has been investigated. For example, Nuchitprasitchai et al. developed a camera-based error detection system [69,70]. In this research, two different systems with either a single-camera and double-camera setup were built. For the single-camera error detection system, the error is detected by comparing the STL image (2D profile extracted from the 3D STL file) with the camera image (2D image captured from the 3D printing product). After rescaling, a printing error is considered as a defect if the differences calculated by subtracting the STL image from the camera image are over 5%. To detect the printing error with the two-camera system, a 3D reconstruction product image was built. For this setup, the printed error between the 3D reconstruction product image and the 3D printed product is detected. If the difference is more than 5%, in which case, an action is taken to stop the printing. A profile monitoring based FFF product quality control approach was proposed by He et al. [91]. The product dimension deviation is obtained by comparing the built profile with the CAD profile layer by layer. The designed system could detect defects, such as dislocation, staircase, and gradual change.

More complex multi-camera systems have also been developed. Straub et al. built a multi-camera system that could achieve full image coverage of the product [72]. An imaging processing technique is applied in this research that compared images taken during the product printing progress to expected product images (e.g., CAD files) to assess the printing process. The system demonstrated a capability for detecting product defects. Fig. 14 shows the images of different printing stages and the pixel difference between the in-process image and the final product. Fig. 14a shows the finished object image. The partial object displays in Fig. 14b. Fig. 14c and Fig. 14d depicts the partial-complete difference comparison and threshold-exceeding pixels identification. By calculating the aggregate level of the pixel difference between the in-process image with the final product one, just as shown in Fig. 14, the system could detect the incomplete failure. Another error detection system was also developed by Nuchitprasitchai et al., which uses six web cameras to achieve 360 degrees coverage for printed product monitoring [71]. The printing error can be calculated in both the horizontal and vertical magnitude directions by comparing the current printing layer's 3-D reconstruction images with STL image models. Moreover, printing errors such as extruder clogging, filament runout, and incomplete product print can be automatically detected by checking the difference between 3-D reconstruction images and STL model images. The non-rescale and rectification image pre-processing technique in this study has a faster computation speed, and the detection accuracy can achieve 100%.

Laser scanning technology, which has high measurement accuracy and resolution, has also been implemented into 3D printing process monitoring. Comparing the point cloud from the laser scanning with the CAD model, the product geometry error can be recognized. Lin et al. proposed an online quality monitoring system for the material extrusion AM process, based on laser scanning technology [107]. There are three steps to detect the defects: (1) point cloud processing; (2) the comparison process between the CAD data with the scan data; and (3) defect reconstruction process. The proposed system not only effectually detects the underfill defect (e.g., gaps in the thin wall, under-extrusion, and unfinished product) and overfill defect (e.g., over-extrusion and scars) but also can reconstruct the 3D defect model. By combining the laser-scanned coordinates dataset with the self-organizing map (SOM) unsupervised machine learning approach, Khanzadeh et al. presented an approach to quantify the FFF printed product geometric deviation [106]. The geometric deviation is gotten from a comparison between the laser-scanned data with the original CAD data. With the SOM cluster, the geometric deviation on magnitude (severity) and direction can be recognized. Rao et al. proposed a spectral graph theory (SGT) method to quantify the complex AM product dimension deviation [109]. An SGT method achieves the dimensional integrity monitoring by calculating the deviation value based on the normal distance from a point on the 3D point cloud to the CAD model's closest surface. Tootooni et al. built a ML dimensional variation classification method [104]. The spectral graph Laplacian eigenvalues are utilized to extract the features from the laser-scanned 3D point cloud data. Afterward, six ML algorithms (sparse representation, k-nearest neighbors, neural network, naive Bayes, support vector machine, and decision tree) are applied to evaluate the classification accuracy. The result shows that the sparse representation algorithm obtains the best classification accuracy (F1-score > 97%).

In addition to the point cloud generated from the laser scanning, the point cloud from G-code has also been investigated. Holzmond et al. presented a quality assurance system named "certify-as-you-build" [92]. This system obtains product geometry using a three-dimensional digital image correlation (3D-DIC) and then compares the obtained product geometry with the point cloud generated from the G-code command to detect the defects. The local defect (e.g., filament blob) and global defect (e.g., low flow) can be detected and located. Lastly, Kopsacheilis et al. presented an in situ vision-based monitoring system for FFF [95]. By comparing the theoretical point cloud 3D model generated from the G-code command with the reconstructed printed model obtained from the camera, the system is able to evaluate the product accuracy in real-time.

Augmented vision is an emerging technology that has recently been applied to monitoring 3D printer product geometry quality. Ceruti et al. developed an error detection system by applying augmented vision [66]. In this system, a virtual product to be printed is matched to the actual one, so the product geometry in different printing stages can be monitored. If manufacturing errors are detected, the printing process could then be stopped automatically or by the operator. Malik et al. proposed a novel scan-based real-time layer-by-layer monitoring system for the AM process [96]. To reconstruct the 3D model, the printing process image is converted to a 3D file OBJ format. By viewing the generated OBJ file through augmented reality, defects can be clearly visualized.

To improve the product dimension accuracy in FFF, various models

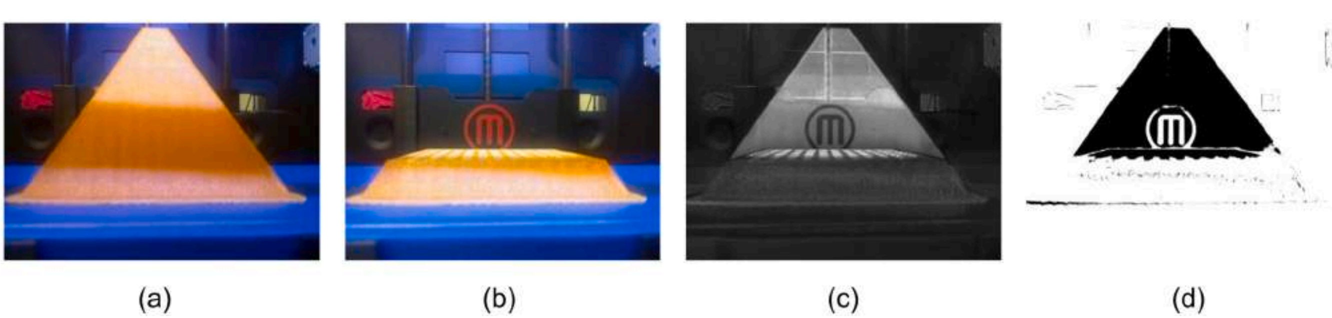

Fig. 14. Images from one angle: (a) the completed product image; (b) the partial product; (c) and (d) the partial-complete difference comparison and threshold-exceeding pixels identification [72].

related to the printing parameters have been built. Boschetto et al. defined a mathematical formulation, which is related to layer thickness and deposition angle, and can be used as a guide for compensating dimensional derivations [198]. With this method, it is possible to get a product with good dimension accuracy without removing the physical error source. In three study cases, the model has a marked dimension deviation reduction. Kaveh et al. investigated how printing parameters affect the product precision and internal cavity for the material without knowing the printing parameters [199]. Then, the presented method tries to find the optimum extruder temperature and raster width settings. The demonstration shows that with the optimized printing parameters, the printed product internal cavity is negligible. Alizadeh et al. built a data-driven model that combines energy consumption with product geometric accuracy [200]. In this research, thickness deviation, product's out-of-tolerance percentage, build time, and energy consumption are selected as the variables. The proposed method is demonstrated and validated its effectiveness by printing on FFF product.

The prediction of a final product's dimension accuracy has also been performed using monitored or known printing parameters. To predict the product dimension deviation for the FFF process, Boschetto et al. developed a model [201] that uses the layer thickness and build orientation as inputs. The prediction value from this model shows a good fit with the experimental data. Noriega et al. proposed a model for predicting the actual printing product dimensions based on the designed characteristics [202]. An artificial neural network is used to predict the actual dimension values; then, an optimization algorithm applies to decide the CAD model's optimal dimensional values. Based on the optimal dimensional values, the CAD model is redesigned. The experimental result shows this methodology could reduce the external dimension error around 50% and internal dimension error around 30%. Yang et al. established a FFF product precision prediction model, which is based on printing process parameters [203]. The input process parameters data is the cable width offset, layer thickness, filling speed, extrusion speed, and the fallback speed. A cyber-model based on printing settings was developed by Miao et al. to predict the deformation during the FFF process [34]. The prediction experiment shows that the linear regression (LN) model performs best compared with the SVM and artificial neural network model. Based on this LN model, a cyber-physical system (CPS) was developed, which could adjust the nozzle temperature automatically. The evaluation experiment indicates this CPS could reduce the distortion remarkably. Song et al. addressed a shape deviation model for the FFF process [204]. In this research, the author attributes the extruder position error and processing error, including phase change and other occurred variation as two error sources, which impact the product consecutively. The Kriging method is applied to predict the extruder position error pattern. Both the experimental and case study shows that the proposed model could successfully grasp the deviation trend. Hebda et al. presented a method to predict the product geometric characteristics for the FFF process [205]. Base on the proposed equations, the product height, width, and cross-section area can be predicted for the given printing parameters.

4. Conclusion and future trends

FFF is the most commonly used 3D printing method due to its advantages of low production cost and the ability to create complicated geometries and shapes. However, its lower reliability means that significant work has been undertaken for the in situ monitoring of FFF as a first step to enabling robust closed-loop control of the FFF process. This paper summarized recent research focused on the in situ monitoring system for the FFF process. In situ monitoring is a driver for the next-generation of systems and polymers in AM. Their implementation will continue to increase the quality, efficiency, and sustainability of polymer components manufactured using the FFF process.

Sensing systems play a key role in the success of in situ monitoring systems. While indirect sensing methods (e.g., vibration and acoustic emissions) are useful for detecting whether a system is experiencing a fault, their ability to link a signal to a specific fault source is limited by the "uniqueness" in their signal. The "uniqueness" issue for indirect sensing methods represents a significant knowledge gap that limits the use of indirect sensing methods for in situ monitoring. Thermal and optical cameras are the most common method for in situ monitoring and have demonstrated success in fault detection, localization, and quantification.

A multitude of data-driven methods for detection printer fault scenarios have been developed, however, the issue with "uniqueness" in their signal remains. Model-based and data-driven approaches for the in situ monitoring of components during printing have also been developed. These methods have demonstrated success in detecting geometry and surface roughness errors.

Great progress has been made in the field of in situ monitoring for the FFF process. However, a knowledge gap still exists in how to use the information gained for the advancement of the FFF process in industrial manufacturing settings. Most importantly, the use of in situ monitoring for structural fault detection in components is yet to be realized. Structural faults are those that limit the structural functionality of a component, rather than just detecting faults related to component geometry or surface roughness that presently obtains. If structural fault detection can be widely achieved, the results could be integrated into part validation methodologies to empower in situ validation, with limited destructive or non-destructive testing of components post-print. Component validation using in situ monitoring would provide a significant forward leap to the FFF process. While data-driven approaches for structural fault detection may be relatively easy to develop, their "black box" approach makes them challenging to integrate into validation procedures for critical components. Model-based and or physics-based approaches that directly consider the thermodynamic and kinetic states of the component during the manufacturing process will allow for direct fault detection, localization, and quantification. Therefore, it is envisioned that the model-based approaches offer the most realistic approach to achieving in situ component validation.

A unified framework that can flexibly integrate available sensors, algorithms and computational models will truly accelerate technology advancement. In the foreseeable future, the FFF system will be realized without a human-in-the-loop [104,184,206]. Moreover, the ability to detect and prevent cyber attacks in real-time offers a path forward for future research [193,207,208].

Declaration of Competing Interest

The authors declare that they have no known competing financial interests or personal relationships that could have appeared to influence the work reported in this paper.

Acknowledgments

This material is based upon work supported by the South Carolina Research Authority under grant 30228 and the South Carolina Space Grant Consortium under grant 521179-RP-SC007. The support of these agencies is gratefully acknowledged. Any opinions, findings, and conclusions or recommendations expressed in this material are those of the authors and do not necessarily reflect the views of the South Carolina Research Authority or the South Carolina Space Grant Consortium. Distribution Statement A. Approved for public release: distribution unlimited.

References

[1] Samuel H. Huang, Peng Liu, Abhiram Mokasdar, Liang Hou, Additive manufacturing and its societal impact: a literature review, Int. J. Adv. Manuf. Technol. 67 (5–8) (2012) 1191–1203.

[2] Yong Huang, Ming C. Leu, Jyoti Mazumder, Alkan Donmez, Additive manufacturing: current state, future potential, gaps and needs, and recommendations, J. Manuf. Sci. Eng. 137 (1) (2015), 014001.
[3] I. Campbell, O. Campbell, R. Huff, J. Kowen, Wohlers report 2020: 3d Printing and Additive Manufacturing State of the Industry, Wohlers Associates, 2020.
[4] Nayanee Gupta, Christopher Weber, Sherrica Newsome, Additive Manufacturing: Status and Opportunities, Science and Technology Policy Institute, Washington, 2012.
[5] N. Mohan, P. Senthil, S. Vinodh, N. Jayanth, A review on composite materials and process parameters optimisation for the fused deposition modelling process, Virtual Phys. Prototyp. 12 (1) (2017) 47–59.
[6] Bettina Wendel, Dominik Rietzel, Florian Kühnlein, Robert Feulner, Gerrit Hülder, Ernst Schmachtenberg, Additive processing of polymers, Macromol. Mater. Eng. 293 (10) (2008) 799–809.
[7] Bethany C. Gross, Jayda L. Erkal, Sarah Y. Lockwood, Chengpeng Chen, Dana M. Spence, Evaluation of 3d printing and its potential impact on biotechnology and the chemical sciences, Anal. Chem. 86 (7) (2014) 3240–3253.
[8] Mostafa Yossef, An Chen.Applicability and limitations of 3d printing for civil structures, 2015.
[9] C. Lee Ventola, Medical applications for 3d printing: current and projected uses, Pharm. Ther. 39 (10) (2014) 704.
[10] Mark H. Michalski, Joseph S. Ross, The shape of things to come: 3d printing in medicine, J. Am. Med. Assoc. 312 (21) (2014) 2213–2214.
[11] Robin P.G. Tech, Jan-Peter Ferdinand, Martina Dopfer, Open source hardware startups and their communities. The Cecentralized and Networked Future of Value Creation, Springer, 2016, pp. 129–145.
[12] Simon Ford, Tim Minshall, Invited review article: where and how 3d printing is used in teaching and education, Addit. Manuf. 25 (2019) 131–150.
[13] Paul Francis Jacobs, Rapid Prototyping & Manufacturing: Fundamentals of Stereolithography, Society of Manufacturing Engineers, 1992.
[14] Joseph J. Beaman, John W. Barlow, David L. Bourell, Richard H. Crawford, Harris L. Marcus, Kevin P. McAlea, Solid Freeform Fabrication: A New Direction in Manufacturing, 2061, Kluwer Academic Publishers, Norwell, MA, 1997, pp. 25–49.
[15] Michael Feygin, Brian Hsieh.Laminated object manufacturing (lom): a simpler process. In 1991 International Solid Freeform Fabrication Symposium, 1991.
[16] B.T. Wittbrodt, A.G. Glover, J. Laureto, G.C. Anzalone, D. Oppliger, J.L. Irwin, J. M. Pearce, Life-cycle economic analysis of distributed manufacturing with open-source 3-d printers, Mechatronics 23 (6) (2013) 713–726.
[17] L. Villalpando, Hasti Eiliat, Ruth Jill Urbanic, An optimization approach for components built by fused deposition modeling with parametric internal structures, Procedia CIRP 17 (2014) 800–805.
[18] Pulak M. Pandey, N.Venkata Reddy, Sanjay G. Dhande, Improvement of surface finish by staircase machining in fused deposition modeling, J. Mater. Process. Technol. 132 (1–3) (2003) 323–331.
[19] L.M. Galantucci, F. Lavecchia, G. Percoco, Experimental study aiming to enhance the surface finish of fused deposition modeled parts, CIRP Ann. 58 (1) (2009) 189–192.
[20] Kalman D. Migler, Richard E. Ricker, Measurement science roadmap for polymer-based additive manufacturing. Technical report, 2016.
[21] Matthew Fiedler, Evaluating tension and tooth geometry to optimize grip on 3d printer filament, 3D Print. Addit. Manuf. 2 (2) (2015) 85–88.
[22] N. Volpato, D. Kretschek, JA Foggiatto, CM GomezdaSilvaCruz, Experimental analysis of an extrusion system for additive manufacturing based on polymer pellets, Int. J. Adv. Manuf. Technol. 81 (9–12) (2015) 1519–1531.
[23] Yuan Cheng, Mohsen A. Jafari, Vision-based online process control in manufacturing applications, IEEE Trans. Autom. Sci. Eng. 5 (1) (2008) 140–153.
[24] Chenang Liu, Andrew Chung Chee Law, David Roberson, Zhenyu (James) Kong, Image analysis-based closed loop quality control for additive manufacturing with fused filament fabrication, J. Manuf. Syst. 51 (75–86) (2019).
[25] David A. Anderegg, Hunter A. Bryant, Devante C. Ruffin, Stephen M. Skrip Jr, Jacob J. Fallon, Eric L. Gilmer, Michael J. Bortner, In-situ monitoring of polymer flow temperature and pressure in extrusion based additive manufacturing, Addit. Manuf. 26 (2019) 76–83.
[26] Prahalad K. Rao, Jia Peter Liu, David Roberson, Zhenyu James Kong, Christopher Williams, Online real-time quality monitoring in additive manufacturing processes using heterogeneous sensors, J. Manuf. Sci. Eng. 137 (6) (2015), 061007.
[27] Fang Peng, BryanD. Vogt, Miko Cakmak, Complex flow and temperature history during melt extrusion in material extrusion additive manufacturing, Addit. Manuf. 22 (197–206) (2018).
[28] Kaveh Bastani, Prahalad K. Rao, Zhenyu(James) Kong, An online sparse estimation-based classification approach for real-time monitoring in advanced manufacturing processes from heterogeneous sensor data, IIE Trans. 48 (7) (2015) 579–598.
[29] Timothy J. Coogan, David O. Kazmer, Prediction of interlayer strength in material extrusion additive manufacturing, Addit. Manuf. (2020), 101368.
[30] Michele Moretti, Federico Bianchi, Nicola Senin, Towards the development of a smart fused filament fabrication system using multi-sensor data fusion for in-process monitoring, Rapid Prototyp. J. (2020).
[31] Jungsoo Nam, Nanhyeon Jo, Jung Sub Kim, Sang Won Lee, Development of a health monitoring and diagnosis framework for fused deposition modeling process based on a machine learning algorithm, Proc. Inst. Mech. Eng. Part B J. Eng. Manuf. 234 (1–2) (2019) 324–332.
[32] Zhixiong Li, Ziyang Zhang, Junchuan Shi, Dazhong Wu, Prediction of surface roughness in extrusion-based additive manufacturing with machine learning, Robot. Comput.-Integr. Manuf. 57 (2019) 488–495.
[33] Dazhong Wu, Yupeng Wei, Janis Terpenny, Surface roughness prediction in additive manufacturing using machine learning.In ASME 2018 13th International Manufacturing Science and Engineering Conference. American Society of Mechanical Engineers Digital Collection, 2018.
[34] Guanxiong Miao, Sheng-Jen Hsieh, JA Segura, Jia-Chang Wang, Cyber-physical system for thermal stress prevention in 3d printing process, Int. J. Adv. Manuf. Technol. 100 (1–4) (2019) 553–567.
[35] Felix Baumann, Manuel Schön, Julian Eichhoff, Dieter Roller, Concept development of a sensor array for 3d printer, Procedia CIRP 51 (2016) 24–31.
[36] Timothy J. Coogan, David O. Kazmer, In-line rheological monitoring of fused deposition modeling, J. Rheol. 63 (1) (2019) 141–155.
[37] Jie Liu, Youmin Hu, Bo Wu, Yan Wang, An improved fault diagnosis approach for fdm process with acoustic emission, J. Manuf. Process. 35 (2018) 570–579.
[38] Haixi Wu, Yan Wang, Zhonghua Yu, In situ monitoring of FDM machine condition via acoustic emission, Int. J. Adv. Manuf. Technol. (2015).
[39] Haixi Wu, Zhonghua Yu, Yan Wang, A new approach for online monitoring of additive manufacturing based on acoustic emission.In ASME 2016 11th International Manufacturing Science and Engineering Conference, V003T08A013-V003T08A013.American Society of Mechanical Engineers, 2016.
[40] Haixi Wu, Zhonghua Yu, Yan Wang, Real-time FDM machine condition monitoring and diagnosis based on acoustic emission and hidden semi-markov model, Int. J. Adv. Manuf. Technol. 90 (5–8) (2016) 2027–2036.
[41] Zhensheng Yang, Li Jin, Youruiling Yan, Yiming Mei, Filament breakage monitoring in fused deposition modeling using acoustic emission technique, Sensors 18 (3) (2018) 749.
[42] Jung Sub Kim, Chang Su Lee, Sung-Min Kim, Sang Won Lee, Development of data-driven in-situ monitoring and diagnosis system of fused deposition modeling (fdm) process based on support vector machine algorithm, Int. J. Precis. Eng. Manuf.-Green Technol. 5 (4) (2018) 479–486.
[43] Feng Li, Zhonghua Yu, Xuanwei Shen, Hao Zhang, Status recognition for fused deposition modeling manufactured parts based on acoustic emission, E3S Web Conf. 95 (2019) 01005.
[44] Feng Li, Zhonghua Yu, Zhensheng Yang, Xuanwei Shen, Real-time distortion monitoring during fused deposition modeling via acoustic emission, Struct. Health Monit. 19 (2) (2020) 412–423.
[45] Haixi Wu, Zhonghua Yu, Yan Wang, Experimental study of the process failure diagnosis in additive manufacturing based on acoustic emission, Measurement 136 (2019) 445–453.
[46] Yongxiang Li, Wei Zhao, Qiushi Li, Tongcai Wang, Gong Wang, In-situ monitoring and diagnosing for fused filament fabrication process based on vibration sensors, Sensors 19 (11) (2019) 2589.
[47] Satish Bukkapatnam, Ben Clark, Dynamic modeling and monitoring of contour crafting–an extrusion-based layered manufacturing process, J. Manuf. Sci. Eng. (2006).
[48] Yang Gao, Borui Li, Wei Wang, Wenyao Xu, Chi Zhou, Zhanpeng Jin, Watching and safeguarding your 3d printer, Proceedings of the ACM on Interactive, Mobile, Wearable and Ubiquitous Technologies, 2 (3): 1–27, September 2018.
[49] Yedige Tlegenov, Geok Soon Hong, Wen Feng Lu, Nozzle condition monitoring in 3d printing, Robot. Comput.-Integr. Manuf. 54 (2018) 45–55.
[50] Yedige Tlegenov, Wen Feng Lu, Geok Soon Hong, A dynamic model for current-based nozzle condition monitoring in fused deposition modelling, Prog. Addit. Manuf. 4 (3) (2019) 211–223.
[51] Chiyen Kim, David Espalin, Alejandro Cuaron, Mireya A. Perez, Eric MacDonald, Ryan B. Wicker, A study to detect a material deposition status in fused deposition modeling technology.In 2015 IEEE International Conference on Advanced Intelligent Mechatronics (AIM). IEEE, July 2015.
[52] Wout De Backer, Paul Sinkez, Ishit Chhabra, Michael J. Van Tooren, Arturs Bergs, In-process monitoring of continuous fiber additive manufacturing through force/torque sensing on the nozzle. In AIAA Scitech 2020 Forum, 1632, 2020.
[53] Pavan Bhavsar, Bhisham Sharma, Wilfredo Moscoso-Kingsley, Vis Madhavan, Detecting first layer bond quality during FDM 3d printing using a discrete wavelet energy approach, Procedia Manuf. 48 (2020) 718–724.
[54] S.F. Costa, F.M. Duarte, J.A. Covas, Estimation of filament temperature and adhesion development in fused deposition techniques, J. Mater. Process. Technol. 245 (2017) 167–179.
[55] E. Ferraris, J. Zhang, B. Van Hooreweder, Thermography based in-process monitoring of fused filament fabrication of polymeric parts, CIRP Ann. 68 (1) (2019) 213–216.
[56] Jingran Li, Ran Jin, ZYu Hang, Integration of physically-based and data-driven approaches for thermal field prediction in additive manufacturing, Mater. Des. 139 (2018) 473–485.
[57] Ehsan Malekipour, Samuel Attoye, Hazim El-Mounayri, Investigation of layer based thermal behavior in fused deposition modeling process by infrared thermography, Procedia Manuf. 26 (2018) 1014–1022.
[58] D. Pollard, C. Ward, G. Herrmann, J. Etches, Filament temperature dynamics in fused deposition modelling and outlook for control, Procedia Manuf. 11 (2017) 536–544.
[59] Hardikkumar Prajapati, Darshan Ravoori, Ankur Jain, Measurement and modeling of filament temperature distribution in the standoff gap between nozzle and bed in polymer-based additive manufacturing, Addit. Manuf. 24 (2018) 224–231.

[60] Jonathan E. Seppala, Kalman D. Migler, Infrared thermography of welding zones produced by polymer extrusion additive manufacturing, Addit. Manuf. 12 (2016) 71–76.
[61] Jonathan E. Seppala, Seung Hoon Han, Kaitlyn E. Hillgartner, Chelsea S. Davis, Kalman B. Migler, Weld formation during material extrusion additive manufacturing, Soft Matter 13 (38) (2017) 6761–6769.
[62] Ketai He, Huan Wang, Huaqing Hu, Approach to online defect monitoring in fused deposition modeling based on the variation of the temperature field, Complexity 2018 (2018) 1–13.
[63] Huaqing Hu, Ketai He, Tianlin Zhong, Yili Hong, Fault diagnosis of fdm process based on support vector machine (svm), Rapid Prototyp. J. (2019).
[64] Felix Baumann, Dieter Roller, Vision based error detection for 3d printing processes.MATEC Web of Conferences, 59: 06003, 2016.
[65] Gabriel Pieter Greeff, Meinhard Schilling, Closed loop control of slippage during filament transport in molten material extrusion, Addit. Manuf. 14 (2017) 31–38.
[66] Alessandro Ceruti, Alfredo Liverani, Tiziano Bombardi, Augmented vision and interactive monitoring in 3d printing process, Int. J. Interact. Des. Manuf. 11 (2) (2017) 385–395.
[67] Ugandhar Delli, Shing Chang, Automated process monitoring in 3d printing using supervised machine learning, Procedia Manuf. 26 (2018) 865–870.
[68] Zeqing Jin, Zhizhou Zhang, Grace X. Gu, Autonomous in-situ correction of fused deposition modeling printers using computer vision and deep learning, Manuf. Lett. 22 (2019) 11–15.
[69] Siranee Nuchitprasitchai, An algorithm for reconstructing three-dimensional images from overlapping two-dimensional intensity measurements with relaxed camera positioning requirements, with application to additive manufacturing, 2017.
[70] Siranee Nuchitprasitchai, Michael Roggemann, Joshua M. Pearce, Factors effecting real-time optical monitoring of fused filament 3d printing, Prog. Addit. Manuf. 2 (3) (2017) 133–149.
[71] Siranee Nuchitprasitchai, Michael Roggemann, Joshua Pearce, Three hundred and sixty degree real-time monitoring of 3-d printing using computer analysis of two camera views, J. Manuf. Mater. Process. 1 (1) (2017) 2.
[72] Jeremy Straub, Initial work on the characterization of additive manufacturing (3d printing) using software image analysis, Machines 3 (2) (2015) 55–71.
[73] Mingtao Wu, Vir V. Phoha.Young B. Moon, Amith K. Belman, Detecting malicious defects in 3d printing process using machine learning and image classification. In ASME 2016 International Mechanical Engineering Congress and Exposition. American Society of Mechanical Engineers Digital Collection, 2016.
[74] Krzysztof Okarma, Jaroslaw Fastowicz, Adaptation of full-reference image quality assessment methods for automatic visual evaluation of the surface quality of 3d prints, Elektron. Elektrotech. 25 (5) (2019) 57–62.
[75] Krzysztof Okarma, Jarosław Fastowicz, Mateusz Tecław, Application of structural similarity based metrics for quality assessment of 3d prints. Computer Vision and Graphics, Springer International Publishing, 2016, pp. 244–252.
[76] Krzysztof Okarma, Jarosław Fastowicz.No-reference quality assessment of 3d prints based on the glcm analysis.In 2016 21st International Conference on Methods and Models in Automation and Robotics (MMAR), 788–793.IEEE, 2016.
[77] Krzysztof Okarma, Jarosław Fastowicz, Color independent quality assessment of 3d printed surfaces based on image entropy. Advances in Intelligent Systems and Computing, Springer International Publishing, 2017, pp. 308–315.
[78] Jeremy Straub, Identifying positioning-based attacks against 3d printed objects and the 3d printing process, in: Pattern Recognition and Tracking XXVIII, 10203, International Society for Optics and Photonics, 2017, p. 1020304.
[79] Jarosław Fastowicz, Marek Grudziński, Mateusz Tecław, Krzysztof Okarma, Objective 3d printed surface quality assessment based on entropy of depth maps, Entropy 21 (1) (2019) 97.
[80] Jaros law Fastowicz, Krzysztof Okarma, Quality assessment of photographed 3d printed flat surfaces using hough transform and histogram equalization, J. Univers. Comput. Sci. 25 (6) (2019) 701–717.
[81] Jeremy Straub, An approach to detecting deliberately introduced defects and micro-defects in 3d printed objects, in: Pattern Recognition and Tracking XXVIII, 10203, International Society for Optics and Photonics, 2017, p. 102030L.
[82] Jeremy Straub, Physical security and cyber security issues and human error prevention for 3d printed objects: detecting the use of an incorrect printing material, in: Dimensional Optical Metrology and Inspection for Practical Applications VI, 10220, International Society for Optics and Photonics, 2017, p. 102200K.
[83] Sam Hurd, Carmen Camp, Jules White, Quality assurance in additive manufacturing through mobile computing. Lecture Notes of the Institute for Computer Sciences, Social Informatics and Telecommunications Engineering, Springer International Publishing, 2015, pp. 203–220.
[84] Krzysztof Okarma, Jarosław Fastowicz, Computer vision methods for non-destructive quality assessment in additive manufacturing. In International Conference on Computer Recognition Systems, 11–20, Springer, 2019.
[85] Okarma Krzysztof, Fastowicz Jarosław, Improved quality assessment of colour surfaces for additive manufacturing based on image entropy, Pattern Anal. Appl. 23 (3) (2020) 1035–1047.
[86] Krzysztof Okarma, Jarosław Fastowicz, Piotr Lech, Vladimir Lukin, Quality assessment of 3d printed surfaces using combined metrics based on mutual structural similarity approach correlated with subjective aesthetic evaluation, Appl. Sci. 10 (18) (2020) 6248.
[87] Jarosław Fastowicz, Krzysztof Okarma, Texture based quality assessment of 3d prints for different lighting conditions. Computer Vision and Graphics, Springer International Publishing, 2016, pp. 17–28.
[88] Jarosław Fastowicz, Krzysztof Okarma, Automatic colour independent quality evaluation of 3d printed flat surfaces based on clahe and hough transform. In International Conference on Image Processing and Communications, 123–131. Springer, 2018.
[89] Jarosław Fastowicz, Piotr Lech, Krzysztof Okarma, Combined metrics for quality assessment of 3d printed surfaces for aesthetic purposes: Towards higher accordance with subjective evaluations. In International Conference on Computational Science, 326–339. Springer, 2020.
[90] Yaser Banadaki, Nariman Razaviarab, Hadi Fekrmandi, Safura Sharifi, Toward enabling a reliable quality monitoring system for additive manufacturing process using deep convolutional neural networks.arXiv preprint arXiv:2003.08749, 2020.
[91] Ketai He, Qian Zhang, Yili Hong, Profile monitoring based quality control method for fused deposition modeling process, J. Intell. Manuf. 30 (2) (2018) 947–958.
[92] Oliver Holzmond, Xiaodong Li, In situ real time defect detection of 3d printed parts, Addit. Manuf. 17 (2017) 135–142.
[93] Tingting Huang, Shanggang Wang, Shunkun Yang, Wei Dai, Statistical process monitoring in a specified period for the image data of fused deposition modeling parts with consistent layers, J. Intell. Manuf. (2020).
[94] Zeqing Jin, Zhizhou Zhang, Grace X. Gu, Automated real-time detection and prediction of interlayer imperfections in additive manufacturing processes using artificial intelligence, Adv. Intell. Syst. 2 (1) (2019), 1900130.
[95] Charalampos Kopsacheilis, Paschalis Charalampous, Ioannis Kostavelis, Dimitrios Tzovaras, In situ visual quality control in 3d printing. In Proceedings of the 15th International Joint Conference on Computer Vision, Imaging and Computer Graphics Theory and Applications. SCITEPRESS - Science and Technology Publications, 2020.
[96] Ammar Malik, Hugo Lhachemi, Joern Ploennigs, Amadou Ba, Robert Shorten, An application of 3d model reconstruction and augmented reality for real-time monitoring of additive manufacturing, Procedia CIRP 81 (2019) 346–351.
[97] Marc Preissler, Chen Zhang, Maik Rosenberger, Gunther Notni, Platform for 3d inline process control in additive manufacturing, in: Peter Lehmann, Wolfgang Osten, Armando Albertazzi Gonçalves (Eds.), Optical Measurement Systems for Industrial Inspection X, SPIE, 2017.
[98] Aditya Saluja, Jiarui Xie, Kazem Fayazbakhsh, A closed-loop in-process warping detection system for fused filament fabrication using convolutional neural networks, J. Manuf. Process. 58 (2020) 407–415.
[99] Yuanbin Wang, Jiakang Huang, Yuan Wang, Sihang Feng, Tao Peng, Huayong Yang, Jun Zou, A CNN-based adaptive surface monitoring system for fused deposition modeling, IEEE/ASME Trans. Mechatron. (2020).
[100] Wu Yi, He Ketai, Zhou Xiaomin, Ding Wenying, Machine vision based statistical process control in fused deposition modeling. In 2017 12th IEEE Conference on Industrial Electronics and Applications (ICIEA). IEEE, June 2017.
[101] Yi WU, Ketai HE, Huaqing HU, Xue ZHAO, Process monitoring of fused deposition modeling through profile control. In 2018 IEEE International Conference on Cyborg and Bionic Systems (CBS). IEEE, October 2018.
[102] Zhicheng Zhang, Ismail Fidan, Michael Allen, Detection of material extrusion in-process failures via deep learning, Inventions 5 (3) (2020) 25.
[103] L. Li, R. McGuan, P. Kavehpour, R.N. Candler, Precision enhancement of 3d printing via in situ metrology.Solid Freeform Fabrication Symposium – An Additive Manufacturing Conference, 2018.
[104] M. Samie Tootooni, Ashley Dsouza, Ryan Donovan, Prahalad K. Rao, Zhenyu James Kong, Peter Borgesen, Classifying the dimensional variation in additive manufactured parts from laser-scanned three-dimensional point cloud data using machine learning approaches, J. Manuf. Sci. Eng. 139 (9) (2017), 091005.
[105] Matthias Faes, Wim Abbeloos, Frederik Vogeler, Hans Valkenaers, Kurt Coppens, Toon Goedemé, Eleonora Ferraris, Process monitoring of extrusion based 3d printing via laser scanning.arXiv preprint arXiv:1612.02219, 2016.
[106] Mojtaba Khanzadeh, Prahalada Rao, Ruholla Jafari-Marandi, Brian K. Smith, Mark A. Tschopp, Linkan Bian, Quantifying geometric accuracy with unsupervised machine learning: using self-organizing map on fused filament fabrication additive manufacturing parts, J. Manuf. Sci. Eng. 140 (3) (2018).
[107] Weiyi Lin, Hongyao Shen, Jianzhong Fu, Senyang Wu, Online quality monitoring in material extrusion additive manufacturing processes based on laser scanning technology, Precis. Eng. 60 (2019) 76–84.
[108] George Papazetis, George-Christopher Vosniakos, Mapping of deposition-stable and defect-free additive manufacturing via material extrusion from minimal experiments, Int. J. Adv. Manuf. Technol. 100 (9) (2019) 2207–2219.
[109] Prahalad K. Rao, Zhenyu Kong, Chad E. Duty, Rachel J. Smith, Three dimensional point cloud measurement based dimensional integrity assessment for additive manufactured parts using spectral graph theory. In International manufacturing science and engineering conference, 49903, V002T04A048. American Society of Mechanical Engineers, 2016.
[110] Felix Sohnius, Peter Schlegel, Max Ellerich, Robert H. Schmitt, Data-driven prediction of surface quality in fused deposition modeling using machine learning. Production at the Leading Edge of Technology, Springer Berlin Heidelberg, 2019, pp. 473–481.
[111] David Blanco, Pedro Fernandez, Alvaro Noriega, Braulio J. Alvarez, Gonzalo Valiño, Layer contour verification in additive manufacturing by means of commercial flatbed scanners, Sensors 20 (1) (2020) 1.
[112] Enrique Soriano Heras, Fernando Blaya Haro, José de Agustín del Burgo, ManuelIslán Marcos, Roberto D'Amato, Filament advance detection sensor for fused deposition modelling 3d printers, Sensors 18 (5) (2018) 1495.
[113] Ian Cummings, Elizabeth Hillstrom, Rielly Newton, Eric Flynn, Adam Wachtor, In-process ultrasonic inspection of additive manufactured parts, in: Topics in

Modal Analysis & Testing, 10, Springer International Publishing, 2016, pp. 235–247.
[114] Xiaochi Xu, Chaitanya Krishna Prasad Vallabh, Zachary James Cleland, Cetin Cetinkaya, Phononic crystal artifacts for real-time in situ quality monitoring in additive manufacturing, J. Manuf. Sci. Eng. 139 (9) (2017).
[115] Yanglong Lu, Yan Wang, Monitoring temperature in additive manufacturing with physics-based compressive sensing, J. Manuf. Syst. 48 (2018) 60–70.
[116] Yanglong Lu, Yan Wang, An efficient transient temperature monitoring of fused filament fabrication process with physics-based compressive sensing, IISE Trans. 51 (2) (2019) 168–180.
[117] Yanglong Lu, Yan Wang.An improvement of physics based compressive sensing with domain decomposition to monitor temperature in fused filament fabrication process. In International Manufacturing Science and Engineering Conference, 58745, V001T01A032. American Society of Mechanical Engineers, 2019.
[118] Jiaqiang Li, Huimin Xie, Kang Ma, In-situ monitoring of the deformation during fused deposition modeling process using cgs method, Polym. Test. 76 (2019) 166–172.
[119] Q. Sun, G.M. Rizvi, C.T. Bellehumeur, P. Gu, Effect of processing conditions on the bonding quality of FDM polymer filaments, Rapid Prototyp. J. 14 (2) (2008) 72–80.
[120] David Mathew Roberson III, Sensor-based Online Process Monitoring in Advanced Manufacturing, Virginia Tech, 2016. PhD thesis.
[121] Barath Narayanan, Kelly Beigh, Gregory Loughnane, Nilesh U. Powar, Support vector machine and convolutional neural network based approaches for defect detection in fused filament fabrication, in: Michael E. Zelinski, Tarek M. Taha, Jonathan Howe, Abdul A. Awwal, Khan M. Iftekharuddin (Eds.), Applications of Machine Learning, SPIE, 2019.
[122] Mostafa Yakout, M.A. ElbestawiStephen, Stephen C. Veldhuis, A review of metal additive manufacturing technologies, Solid State Phenom. 278 (2018) 1–14.
[123] Yuen-Shan Leung, Tsz-Ho Kwok, Xiangjia Li, Yang Yang, Charlie C.L. Wang, Yong Chen, Challenges and status on design and computation for emerging additive manufacturing technologies, J. Comput. Inf. Sci. Eng. 19 (2) (2019).
[124] Hoejin Kim, Yirong Lin, Tzu-Liang Bill Tseng, A review on quality control in additive manufacturing, Rapid Prototyp. J. 24 (3) (2018) 645–669.
[125] T. DebRoy, H.L. Wei, J.S. Zuback, T. Mukherjee, J.W. Elmer, J.O. Milewski, A. M. Beese, A. Wilson-Heid, A. De, W. Zhang, Additive manufacturing of metallic components — process, structure and properties, Prog. Mater. Sci. 92 (2018) 112–224.
[126] Neng Li, Shuai Huang, Guodong Zhang, Renyao Qin, Wei Liu, Huaping Xiong, Gongqi Shi, Jon Blackburn, Progress in additive manufacturing on new materials: a review, J. Mater. Sci. Technol. 35 (2) (2019) 242–269.
[127] Syed A.M. Tofail, Elias P. Koumoulos, Amit Bandyopadhyay, Susmita Bose, Lisa O'Donoghue, Costas Charitidis, Additive manufacturing: scientific and technological challenges, market uptake and opportunities, Mater. Today 21 (1) (2018) 22–37.
[128] K. Satish Prakash, T. Nancharaih, VV Subba Rao, Additive manufacturing techniques in manufacturing-an overview, Mater. Today. Proc. 5 (2) (2018) 3873–3882.
[129] A. Mitchell, U. Lafont, M. Hołyńska, C. Semprimoschnig, Additive manufacturing — a review of 4d printing and future applications, Addit. Manuf. 24 (2018) 606–626.
[130] Kaufui V. Wong, Aldo Hernandez, A review of additive manufacturing, ISRN Mech. Eng. 2012 (2012) 1–10.
[131] Flaviana Calignano, Diego Manfredi, Elisa Paola Ambrosio, Sara Biamino, Mariangela Lombardi, Eleonora Atzeni, Alessandro Salmi, Paolo Minetola, Luca Iuliano, Paolo Fino, Overview on additive manufacturing technologies, Proc. IEEE 105 (4) (2017) 593–612.
[132] Mariano Jiménez, Luis Romero, Iris A. Domínguez, María del Mar Espinosa, Manuel Domínguez, Additive manufacturing technologies: an overview about 3d printing methods and future prospects, Complexity 2019 (2019) 1–30.
[133] Pedram Parandoush, Dong Lin, A review on additive manufacturing of polymer-fiber composites, Compos. Struct. 182 (2017) 36–53.
[134] Tuan D. Ngo, Alireza Kashani, Gabriele Imbalzano, Kate T.Q. Nguyen, David Hui, Additive manufacturing (3d printing): a review of materials, methods, applications and challenges, Compos. Part B Eng. 143 (2018) 172–196.
[135] Julien Gardan, Additive manufacturing technologies: state of the art and trends, Int. J. Prod. Res. 54 (10) (2015) 3118–3132.
[136] Jodie N. Haigh, Tim R. Dargaville, Paul D. Dalton, Additive manufacturing with polypropylene microfibers, Mater. Sci. Eng. C 77 (2017) 883–887.
[137] Jingchao Jiang, Xun Xu, Jonathan Stringer, Support structures for additive manufacturing: a review, J. Manuf. Mater. Process. 2 (4) (2018) 64.
[138] Diana Popescu, Aurelian Zapciu, Catalin Amza, Florin Baciu, Rodica Marinescu, FDM process parameters influence over the mechanical properties of polymer specimens: a review, Polym. Test. 69 (2018) 157–166.
[139] J.M. Chacón, M.A. Caminero, E. García-Plaza, P.J. Núñez, Additive manufacturing of PLA structures using fused deposition modelling: effect of process parameters on mechanical properties and their optimal selection, Mater. Des. 124 (2017) 143–157.
[140] Muhammad Harris, Johan Potgieter, Richard Archer, Khalid Mahmood Arif, Effect of material and process specific factors on the strength of printed parts in fused filament fabrication: a review of recent developments, Materials 12 (10) (2019) 1664.
[141] International Organization for Standardization, Additive Manufacturing: General: Principles: Terminology, ISO, 2015.
[142] Mohammad Vaezi, Chee Kai Chua, Effects of layer thickness and binder saturation level parameters on 3d printing process, Int. J. Adv. Manuf. Technol. 53 (1–4) (2010) 275–284.
[143] Michael E. Mackay, Zachary R. Swain, Colby R. Banbury, David D. Phan, David A. Edwards, The performance of the hot end in a plasticating 3d printer, J. Rheol. 61 (2) (2017) 229–236.
[144] Md Hazrat Ali, Nazim Mir-Nasiri, Wai Lun Ko, Multi-nozzle extrusion system for 3d printer and its control mechanism, Int. J. Adv. Manuf. Technol. 86 (1–4) (2016) 999–1010.
[145] A. Abilgaziyev, T. Kulzhan, N. Raissov, Md Hazrat Ali, WL KO, N. Mir-Nasiri, Design and development of multi-nozzle extrusion system for 3d printer.In 2015 International Conference on Informatics, Electronics & Vision (ICIEV), 1–5. IEEE, 2015.
[146] Jason Griffey, The types of 3-d printing. Library Technology Reports, 50 (5): 8–12, 2014.
[147] Jamison Go, Scott N. Schiffres, Adam G. Stevens, A. John Hart, Rate limits of additive manufacturing by fused filament fabrication and guidelines for high-throughput system design, Addit. Manuf. 16 (2017) 1–11.
[148] Nicolas G. Morales, Trevor J. Fleck, Jeffrey F. Rhoads, The effect of interlayer cooling on the mechanical properties of components printed via fused deposition, Addit. Manuf. 24 (2018) 243–248.
[149] O.H. Ezeh, L. Susmel, Fatigue behaviour of additively manufactured polylactide (PLA), Procedia Struct. Integr. 13 (2018) 728–734.
[150] Lu Wang, Douglas J. Gardner, Effect of fused layer modeling (FLM) processing parameters on impact strength of cellular polypropylene, Polymer 113 (2017) 74–80.
[151] Lexey R. Sbriglia, Andrew M. Baker, James M. Thompson, Robert V. Morgan, Adam J. Wachtor, John D. Bernardin, Embedding sensors in fdm plastic parts during additive manufacturing, in: Topics in Modal Analysis & Testing, 10, Springer, 2016, pp. 205–214.
[152] Giselle Hsiang Loh, Eujin Pei, Joamin Gonzalez-Gutierrez, Mario Monzón, An overview of material extrusion troubleshooting, Appl. Sci. 10 (14) (2020) 4776.
[153] Shahriar Bakrani Balani, France Chabert, Valérie Nassiet, Arthur Cantarel, Influence of printing parameters on the stability of deposited beads in fused filament fabrication of poly(lactic) acid, Addit. Manuf. 25 (2019) 112–121.
[154] Steven Eric Zeltmann, Nikhil Gupta, Nektarios Georgios Tsoutsos, Michail Maniatakos, Jeyavijayan Rajendran, Ramesh Karri, Manufacturing and security challenges in 3d printing, JOM 68 (7) (2016) 1872–1881.
[155] R.J. Zaldivar, T.D. Mclouth, G.L. Ferrelli, D.N. Patel, A.R. Hopkins, D. Witkin, Effect of initial filament moisture content on the microstructure and mechanical performance of ULTEM® 9085 3d printed parts, Addit. Manuf. 24 (2018) 457–466.
[156] Eric L. Gilmer, Darren Miller, Camden A. Chatham, Callie Zawaski, Jacob J. Fallon, Allison Pekkanen, Timothy E. Long, Christopher B. Williams, Michael J. Bortner, Model analysis of feedstock behavior in fused filament fabrication: enabling rapid materials screening, Polymer 152 (2018) 51–61.
[157] Ben Wittbrodt, Joshua M. Pearce, The effects of PLA color on material properties of 3-d printed components, Addit. Manuf. 8 (2015) 110–116.
[158] Carolina Cardona, Abigail H. Curdes, Aaron J. Isaacs, Effects of filament diameter tolerances in fused filament fabrication, IU J. Undergrad. Res. 2 (1) (2016) 44–47.
[159] Tian-Ming Wang, Jun-Tong Xi, Ye Jin, A model research for prototype warp deformation in the FDM process, Int. J. Adv. Manuf. Technol. 33 (11–12) (2006) 1087–1096.
[160] Martin Spoerk, Joamin Gonzalez-Gutierrez, Janak Sapkota, Stephan Schuschnigg, Clemens Holzer, Effect of the printing bed temperature on the adhesion of parts produced by fused filament fabrication, Plast. Rubber Compos. 47 (1) (2018) 17–24.
[161] Stephan Bechtel, Mirko Meisberger, Samuel Klein, Tobias Heib, Steven Quirin, Hans-Georg Herrmann, Estimation of the adhesion interface performance in aluminum-pla joints by thermographic monitoring of the material extrusion process, Materials 13 (15) (2020) 3371.
[162] Anna Bellini, Selçuk Güçeri, Mechanical characterization of parts fabricated using fused deposition modeling, Rapid Prototyp. J. 9 (4) (2003) 252–264.
[163] José F. Rodríguez, James P. Thomas, John E. Renaud. Design of fused-deposition abs components for stiffness and strength.125(3): 545–551, 2003.
[164] Lennart Bochmann, Cindy Bayley, Moneer Helu, Robert Transchel, Konrad Wegener, David Dornfeld, Understanding error generation in fused deposition modeling, Surf. Topogr. Metrol. Prop. 3 (1) (2015), 014002.
[165] M. AtifYardimci, Takeshi Hattori, Selcuk I. Guceri, Stephen C. Danforth, Thermal analysis of fused deposition.1997.
[166] A. Boschetto, V. Giordano, F. Veniali, Surface roughness prediction in fused deposition modelling by neural networks, Int. J. Adv. Manuf. Technol. 67 (9–12) (2013) 2727–2742.
[167] Samuel O. Attoye, Study of Fused Deposition Modeling (FDM) 3-D Printing Using Mechanical Testing and Thermography, Purdue University, 2018. PhD thesis.
[168] Jie Zhang, XinZhou Wang, WangWang Yu, YuHe Deng, Numerical investigation of the influence of process conditions on the temperature variation in fused deposition modeling, Mater. Des. 130 (2017) 59–68.
[169] Xunfei Zhou, Sheng-Jen Hsieh, Thermal analysis of fused deposition modeling process using infrared thermography imaging and finite element modeling, in: Thermosense: Thermal Infrared Applications XXXIX, 10214, International Society for Optics and Photonics, 2017, p. 1021409.
[170] RalphB Dinwiddie, LonnieJ Love, John C. Rowe, Real-time process monitoring and temperature mapping of a 3d polymer printing process, in: Thermosense: Thermal Infrared Applications XXXV, 8705, International Society for Optics and Photonics, 2013, p. 87050L.

[171] BiranchiN Panda, K. Shankhwar, Akhil Garg, Zhang Jian, Performance evaluation of warping characteristic of fused deposition modelling process, Int. J. Adv. Manuf. Technol. 88 (5–8) (2017) 1799–1811.
[172] Jingchao Jiang, Chunling Yu, Xun Xu, Yongsheng Ma, Jikai Liu, Achieving better connections between deposited lines in additive manufacturing via machine learning, Math. Biosci. Eng. 17 (4) (2020) 3382.
[173] Martin Spoerk, Clemens Holzer, Joamin Gonzalez-Gutierrez, Material extrusion-based additive manufacturing of polypropylene: a review on how to improve dimensional inaccuracy and warpage, J. Appl. Polym. Sci. 137 (12) (2019) 48545.
[174] Antonio Armillotta, Mattia Bellotti, Marco Cavallaro, Warpage of fdm parts: experimental tests and analytic model, Robot. Comput. -Integr. Manuf. 50 (2018) 140–152.
[175] Mohammad Taufik, Prashant K. Jain, A study of build edge profile for prediction of surface roughness in fused deposition modeling, J. Manuf. Sci. Eng. 138 (6) (2016).
[176] PENG AnHua, XIAO XingMing, Investigation on reasons inducing error and measures improving accuracy in fused deposition modeling, Int. J. Adv. Inf. Sci. Serv. Sci. 4 (5) (2012) 149–157.
[177] Yu an Jin, Hui Li, Yong He, Jian zhong Fu, Quantitative analysis of surface profile in fused deposition modelling, Addit. Manuf. 8 (2015) 142–148.
[178] D. Chaidas, K. Kitsakis, J. Kechagias, S. Maropoulos, The impact of temperature changing on surface roughness of fff process. In IOP Conf. Ser. Mater. Sci. Eng, 161, 012033, 2016.
[179] Stephen O. Akande, Dimensional accuracy and surface finish optimization of fused deposition modelling parts using desirability function analysis, Int. J. Eng. Res. Technol. 4 (4) (2015) 196–202.
[180] Daekeon Ahn, Jin-Hwe Kweon, Soonman Kwon, Jungil Song, Seokhee Lee, Representation of surface roughness in fused deposition modeling, J. Mater. Process. Technol. 209 (15–16) (2009) 5593–5600.
[181] Farzaneh Kaji, Ahmad Barari, Evaluation of the surface roughness of additive manufacturing parts based on the modelling of cusp geometry, IFAC-PapersOnLine 48 (3) (2015) 658–663.
[182] Yusuf S. Dambatta, AD Ahmed Sarhan, Surface roughness analysis, modelling and prediction in fused deposition modelling additive manufacturing technology, Int. J. Mech. Aerosp. Ind. Mechatron. Manuf. Eng. 10 (8) (2016) 1568–1575.
[183] Ebrahim Vahabli, Sadegh Rahmati, Hybrid estimation of surface roughness distribution in FDM parts using analytical modeling and empirical investigation, Int. J. Adv. Manuf. Technol. 88 (5–8) (2016) 2287–2303.
[184] Ebrahim Vahabli, Sadegh Rahmati, Application of an RBF neural network for FDM parts' surface roughness prediction for enhancing surface quality, Int. J. Precis. Eng. Manuf. 17 (12) (2016) 1589–1603.
[185] Barrios, Romero, Decision tree methods for predicting surface roughness in fused deposition modeling parts, Materials 12 (16) (2019) 2574.
[186] L. DiAngelo, P. DiStefano, A. Marzola, Surface quality prediction in fdm additive manufacturing, Int. J. Adv. Manuf. Technol. 93 (9–12) (2017) 3655–3662.
[187] Surface roughness - terminology - part 1: Surface and its parameters.1– 16, 1984.
[188] Alberto Boschetto, Luana Bottini, Francesco Veniali, Integration of fdm surface quality modeling with process design, Addit. Manuf. 12 (2016) 334–344.
[189] Alberto Boschetto, Veronica Giordano, Francesco Veniali, 3d roughness profile model in fused deposition modelling, Rapid Prototyp. J. (2013).
[190] Alberto Boschetto, Luana Bottini, Roughness prediction in coupled operations of fused deposition modeling and barrel finishing, J. Mater. Process. Technol. 219 (2015) 181–192.
[191] L. Sturm, C. Williams, J. Camelio, J. White, R. Parker, Cyber-physical vunerabilities in additive manufacturing systems, Context 7 (2014) (2014) 8.
[192] Christian Lubombo, Michel A. Huneault, Effect of infill patterns on the mechanical performance of lightweight 3d-printed cellular PLA parts, Mater. Today Commun. 17 (2018) 214–228.
[193] Mingtao Wu, Zhengyi Song, Young B. Moon, Detecting cyber-physical attacks in CyberManufacturing systems with machine learning methods, J. Intell. Manuf. 30 (3) (2017) 1111–1123.
[194] James R. Munkres. Topology, Second edition, Prentice Hall, Upper Saddle River, NJ 07458, 2000.
[195] Jeremy Straub, 3d printing cybersecurity: detecting and preventing attacks that seek to weaken a printed object by changing fill level, in: Dimensional Optical Metrology and Inspection for Practical Applications VI, 10220, International Society for Optics and Photonics, 2017, p. 102200O.
[196] Ian Campbell, David Bourell, Ian Gibson, Additive manufacturing: rapid prototyping comes of age, Rapid Prototyp. J. 18 (4) (2012) 255–258.
[197] Michael Rimock, An introduction to the intellectual property law implications of 3d printing, Can. J. Law Technol. 13 (1) (2015).
[198] Alberto Boschetto, Luana Bottini, Design for manufacturing of surfaces to improve accuracy in fused deposition modeling, Robot. Comput.-Integr. Manuf. 37 (2016) 103–114.
[199] Mahdi Kaveh, Mohsen Badrossamay, Ehsan Foroozmehr, ArdeshirHemasian Etefagh, Optimization of the printing parameters affecting dimensional accuracy and internal cavity for hips material used in fused deposition modeling processes, J. Mater. Process. Technol. 226 (2015) 280–286.
[200] Morteza Alizadeh, Mehrnaz Noroozi Esfahani, Wenmeng Tian, Junfeng Ma, Data-driven energy efficiency and part geometric accuracy modeling and optimization of green fused filament fabrication processes, J. Mech. Des. 142 (4) (2020).
[201] Alberto Boschetto, Luana Bottini, Accuracy prediction in fused deposition modeling, Int. J. Adv. Manuf. Technol. 73 (5–8) (2014) 913–928.
[202] A. Noriega, D. Blanco, BJ Alvarez, A. Garcia, Dimensional accuracy improvement of fdm square cross-section parts using artificial neural networks and an optimization algorithm, Int. J. Adv. Manuf. Technol. 69 (9–12) (2013) 2301–2313.
[203] Hua Dong Yang, Sen Zhang, Precision prediction model in fdm by the combination of genetic algorithm and bp neural network algorithm, J. Meas. Eng. 5 (3) (2017) 134–141.
[204] Suoyuan Song, Andi Wang, Qiang Huang, Fugee Tsung, Shape deviation modeling for fused deposition modeling processes. In IEEE International Conference on Automation Science and Engineering (CASE). IEEE, August 2014.
[205] Michael Hebda, Claire McIlroy, Ben Whiteside, Fin Caton-Rose, Phil Coates, A method for predicting geometric characteristics of polymer deposition during fused-filament-fabrication, Addit. Manuf. 27 (2019) 99–108.
[206] P. Stavropoulos, D. Chantzis, C. Doukas, A. Papacharalampopoulos, G. Chryssolouris, Monitoring and control of manufacturing processes: a review, Procedia CIRP 8 (2013) 421–425.
[207] Yang Gao, Borui Li, Wei Wang, Wenyao Xu, Chi Zhou, Zhanpeng Jin, Watching and safeguarding your 3d printer: Online process monitoring against cyber-physical attacks. Proc. ACM Interact. Mob. Wearable Ubiquitous Technol., 2(3), September 2018.
[208] Sunpreet Singh, Gurminder Singh, Chander Prakash, Seeram Ramakrishna, Current status and future directions of fused filament fabrication, J. Manuf. Process. 55 (2020) 288–306.